https://doi.org/10.15388/vu.thesis.195
https://orcid.org/0000-0003-2013-5618

VILNIUS UNIVERSITY

Anatolij
NEČIPORENKO

Mathematical Modeling of Bioreactor Control

DOCTORAL DISSERTATION

Natural Sciences,
Informatics (N 009)

VILNIUS 2021

This dissertation was written between 2016 and 2020 at Vilnius University. This work was partially funded by scholarships from The Research Council of Lithuania (*P-DAP-20-184*), Infobalt Young Researcher Scholarships (2017 and 2020) and *COST* (European Cooperation in Science and Technology) Action *IC1305* in 2018.

Academic supervisor – Prof. Dr. Habil. Feliksas Ivanauskas (Vilnius University, Natural Sciences, Informatics – N 009).
Academic consultant – Prof. Dr. Tadas Meškauskas (Vilnius University, Natural Sciences, Informatics – N 009).

https://doi.org/10.15388/vu.thesis.195
https://orcid.org/0000-0003-2013-5618

VILNIAUS UNIVERSITETAS

Anatolij
NEČIPORENKO

Bioreaktoriaus valdymo matematinis modeliavimas

DAKTARO DISERTACIJA

Gamtos mokslai,
informatika (N 009)

VILNIUS 2021

Disertacija rengta 2016 – 2020 metais Vilniaus universitete. Disertacijos rengimą iš dalies finansavo Lietuvos Mokslo Taryba (stipendija *P-DAP-20-184*), Infobalt (jaunojo mokslininko stipendijos 2017 m. ir 2020 m.), *COST* (angl. European Cooperation in Science and Technology, liet. Europos mokslo ir technologijų bendradarbiavimas) (priemonė *IC1305* 2018 m).

Mokslinis vadovas – prof. habil. dr. Feliksas Ivanauskas (Vilniaus universitetas, gamtos mokslai, informatika – N 009).
Mokslinis konsultantas – prof. dr. Tadas Meškauskas (Vilniaus universitetas, gamtos mokslai, informatika – N 009).

Acknowledgements

Undertaking this PhD has been a truly life-changing experience for me and it would not have been possible without the support and guidance that I received from many people.

First and foremost, I would like to say a very big thank you to my supervisor Prof. Dr. Habil. Feliksas Ivanauskas for all the support and encouragement he gave me during those long months dedicated for my field work and the time spent at Vilnius University. Without his guidance and constant feedback this PhD would not have been achievable.

Many thanks also to Prof. Dr. Tadas Meškauskas who, throughout our numerous discussions while I was a master's student, convinced me that I should pursue my doctoral degree and who made it possible for me to gain teaching experience in Vilnius University.

I greatly appreciate the support received through the collaborative work undertaken with the brightest minds from Vilnius University, Kaunas Technology University and Vytautas Magnus University - Prof. Dr. Habil. Valdas Laurinavičius, Prof. Dr. Habil. Mifodijus Sapagovas, Prof. Dr. (HP) Arvydas Povilaitis, Assoc. Prof. Dr. Jurgita Dabulytė-Bagdonavičienė.

I would also like to say a heartfelt thank you to my Mom, Dad, Brother and Wife for always believing in me and encouraging me to follow my dreams. And, finally, I want to thank Aleksej, Andžejus, Daniel and Dmitrij for helping in whatever way they could during this challenging period.

Summary

The main research topic of this thesis is numerical methods for systems of nonlinear partial differential equations with nonlocal boundary conditions and nonlocal conditions. Systems of reaction-diffusion, convection-reaction-diffusion and convection-reaction equations are considered. This research presents a distinct application of nonlocal boundary conditions in process monitoring and control. Nonlocal conditions are defined as the PID (proportional-integral-derivative controller) control algorithm or a subset of its terms (PI, I).

Mathematical modeling of bioreactor control has been applied in the fields of drug delivery and water denitrification. The distinct feature of the model is the nonlocal boundary condition that combines two different components of the solution containing a double integral in space and time.

The stability of a difference scheme for a reaction-diffusion equation system was analyzed. Eigenvalue spectrum analysis for control and equation system parameters was carried out. Sufficient conditions for numerical algorithm difference scheme stability were obtained.

Santrauka

Pagrindinė šios disertacijos tema yra skaitiniai metodai, skirti spęsti netiesines diferencialinių lygčių sistemas dalinėmis išvestinėmis su nelokaliosiomis kraštinėmis sąlygomis ir nelokaliosiomis sąlygomis. Nagrinėjamos reakcijos-difuzijos, konvekcijos-reakcijos-difuzijos ir konvekcijos-reakcijos lygčių sistemos. Darbe pateikiamas išskirtinis nelokalių kraštinių sąlygų taikymas – procesų valdymas. Nelokaliosios sąlygos aprašytos kaip PID (proporcinis-integralinis-išvestinis valdiklis) valdymo algoritmas ar jo komponentų poaibis (PI, I).

Bioreaktorių valdymo matematinis modeliavimas buvo taikomas vaistų įvedimo ir vandens denitrifikacijos srityse. Išskirtinė modelio savybė yra nelokalioji kraštinė sąlyga, kuri sujungia dvi skirtingas sprendinio komponentes su dvilypiu integralu pagal erdvę ir laiką.

Išanalizuotas reakcijos-difuzijos lygčių sistemos skirtuminės schemos stabilumas. Atlikta valdymo ir lygčių sistemos parametrų tikrinių reikšmių spektro analizė. Buvo gautos pakankamos sąlygos skaitinio algoritmo skirtuminės schemos stabilumui.

Table of Contents

List of Figures

List of Tables

Notation

$\mathscr{D}_S$, $\mathscr{D}_P$ – diffusion coefficient
K_M – Michaelis constant
S – concentration of substrate
P – concentration of product
t – time
$\mathrm{V}_{\mathrm{max}}$ – maximal enzymatic rate

Abbreviations

FDM – finite difference method
PDE – partial differential equation
PID – proportional-integral-derivative controller, feedback control loop mechanism

Introduction

Research context and motivation

Mathematical modeling combined with numerical methods allows scientists to design and evaluate approximate models representing real-world objects without the need of building one. In many cases real-world objects have a variety of parameters. Determination and precise tuning of parameters are the daily tasks of engineers.

Computational or numerical experiments can be much more cheaper compared to the prototype builds. Engineers and computer scientists can model a variety of objects with a wide spectrum of parameters without the need of building one. Resources, time and money can be saved if model parameters are adjusted and evaluated on the computer screen without physical object creation.

Many aspects of chemical, biochemical and other processes around us require some kind of control. In general, the most popular and widely adopted controls are the feedback loop control mechanisms, where processes are controlled by measuring the output parameters while adjusting the input.

In present thesis, mathematical models are constructed using reaction-diffusion, convection-reaction and convection-reaction-diffusion equation systems with Michaelis-Menten kinetics and inhibition. Chemical and biochemical reaction process modeling is subjected to a PID control.

The PID (proportional-integral-derivative) algorithm has been around since the 1930s. It remains the foundation of almost all basic control applications [48]. The PID controller is a simple implementation of feedback. It has the ability to eliminate steady-state offsets through integral action, and it can anticipate the future through derivative action. PID controllers, or even PI controllers, are sufficient for many control problems, particularly when process dynamics are benign and the performance requirements are modest. PID controllers are found in large numbers in all industries. The PID controller is an important ingredient of distributed systems for process control. The controllers are also embedded in many special-purpose control systems. In process control, more than 95 percent of the control loops are of the PID type; most loops are actually PI control. [4]

Research area

Mathematical models in this thesis belong to an intensely studied class of problems, namely differential equations subject to nonlocal boundary conditions and nonlocal conditions.

The studied mathematical models belong to a partial differential equations class and they are commonly used to study a wide variety of aspects w.r.t bioreactor and biosensor applications. A distinctive research area of this work is nonlocal conditions and nonlocal boundary conditions. The present research covers both condition types with the main subject of PID control and its term subset (PI, I).

Historically, the oldest mathematical works on the nonlocal conditions seem to be the book [86] and the article [71]. Here, these conditions are known as the "more general boundary conditions" [92]. These works, however, have not attracted much attention. As far as the author knows, the first mathematical models with nonlocal conditions describing real physical processes appeared in scientific journals in the 1960s [11, 45]. These works, although not immediately, have attracted more consideration in scientific publications, especially in mathematical journals.

Authors in related fields are studying mathematical models with nonlocal conditions or nonlocal boundary conditions which are defined for a single second-order differential equation. One of the first mathematical models proposed for a system of two differential equations subject to nonlocal conditions was published in the monograph [83]. Other authors have proposed a system of diffusion-reaction equations describing the action of the non-steady state biosensor at mixed enzyme kinetics, external and internal diffusion limitation with substrate inhibition [35, 36]. A relatively large number of mathematical models with nonlocal conditions describing real processes in a number of applications have been created over the last few decades. Among notable applications, there are heat conduction, thermoelasticity, hydrodynamics, semiconductor devices, ecology, geophysical flows, population dynamics, electrochemistry, and biotechnology (see [13, 14, 24, 25, 44, 47, 62, 85] and the references therein).

Purpose and objectives of the thesis

The main purpose is to provide mathematical models suitable for the monitoring and control of bioreactor processes (incl. parameters). The control system

is used to adjust the outflow of the bioreactor through manipulation of its input parameters.

The objectives of this thesis are to develop, model and investigate the monitoring and control mechanism for bioreactors, based on nonlocal boundary conditions and nonlocal conditions, and propose original mathematical models and computational methods.

The author studies a system of two nonlinear partial differential equations (PDE) subject to a nonlocal and nonlocal boundary condition. Systems of nonlinear PDEs are widely used for mathematical modeling of bioreactors and biosensors in wide variety of aspects and applications [6].

In order to achieve these objectives, the following research tasks need to be performed:

1. Investigate and develop mathematical models with nonlocal boundary conditions for monitoring and control.

2. Propose a mathematical model and a numerical method for a bioreactor with application in drug delivery.

3. Propose a mathematical model and a numerical method for a denitrification bioreactor.

4. Investigate the stability of a difference scheme for mathematical models.

Research methods and tools

The described control system is based on four mechanisms: the given control function (set-point function), the monitoring signal (integral value, measured process variable), the control signal (computed by the controller), and a *mechanical device* providing the boundary value.

A numerical modeling was performed using a computer program developed by the author in Python programming language with *NumPy*, *SciPy* and *Matplotlib* libraries. The program implements an explicit finite difference scheme using a forward difference at time and a second-order central difference for the space derivative. The integrals were computed by the Simpson's rule.
Computer science methods used for problem solution in this thesis:

1. Numerical solution methods for differential equations.

2. Optimization methods for inverse problem solution.

3. Statistical methods and outlier analysis for experimental datasets.

To meet the high need of computing resources for large-scale problems, the supercomputer of Vilnius University was used.

Scientific novelty of the results

The models presented in this work not only provide a set of PDEs, but also describe the underlying physical process together with its possible applications.

The proposed mathematical models and their variations are applied to the numerical modeling of drug delivery and drainage runoff water denitrification processes both subject to monitoring and control.

The main peculiarity of the present research is a sufficiently detailed explanation of the physical principles that were the basis of the nonlocal and nonlocal boundary condition, which reflects the control (regulation) principle. Both conditions (nonlocal and nonlocal boundary) were defined as the PID controller or its term subset (PI, I).

The collection of published manuscripts and given talks is the result of a continuous scientific research.

1. The mathematical model is distinguished by a nonlocal boundary condition with integral expression binding both derivatives with regard to time and space for a real physical problem (drug delivery).

2. The convection–diffusion–reaction model combined with PID control was applied to monitor drug delivery in an enzyme-containing flow-through bioreactor. The control was performed by adjusting the flow rate based on the drug outflow measurements.

3. The PID controller allows to reduce the impact of fluctuations of pumping, diffusion slowdown and reduction of drug production rate on the drug outflow rate.

4. A mathematical model for flow rate selection for denitrification bioreactor is presented. The peculiar feature is the nonlocal condition representing the control mechanism which is defined as a PI controller.

5. The stability of the difference scheme for reaction-diffusion equation system is analyzed. The obtained results allow to choose the proper coefficients for the numerical algorithm with respect to the difference scheme stability as well as the physical properties.

Statements promoted to defend

1. Proposed reaction–diffusion mathematical model with a nonlocal boundary condition subject to PID control for bioreactor modeling in drug delivery field. A constructed numerical algorithm and a developed computer program were used for modeling.

2. A convection–reaction–diffusion system of PDEs with a nonlocal condition is applied to drug delivery mathematical modeling using a developed computer program for the flow-through pressure controlled bioreactor.

3. Proposed mathematical model containing a system of convection–reaction PDEs with a nonlocal condition alongside with a computer program is applied to the nitrate removal in a woodchip denitrification bioreactor with water flow rate monitoring.

4. Sufficient conditions for numerical algorithm stability of difference scheme for the system of reaction-diffusion equations with a nonlocal boundary condition are obtained by using eigenvalue spectrum analysis for control and equation system parameters using a developed computer program.

Approbation of the results

While preparing this thesis, an article titled *Reaction–diffusion equation with nonlocal boundary condition subject to PID-controlled bioreactor* was published in the journal "Nonlinear Analysis: Modelling and Control". This article describes the modeling of a bioreactor with PID control. A mathematical model with the PID controller constructed as a nonlocal boundary condition was introduced. The author contributed to this work by participating in the mathematical model and numerical algorithm formulation process, programming of the numerical algorithm, performing numerical experiments, and making a contribution to charts and manuscript text.

The second article titled *Drug delivery mathematical modeling for pressure controlled bioreactor* was published in the Journal of Mathematical Chemistry. This article describes the modeling of a bioreactor with PID control. The constructed mathematical model introduces the nonlocal condition with the PID controller. The author contributed to this work by participating in the mathematical model and numerical algorithm formulation process, programming of the

numerical algorithm, performing numerical experiments, making a contribution to charts and manuscript text.

The third article titled *Nitrate removal in Woodchip Denitrification Bioreactor - an approach combining mathematical modelling and PI control* was accepted by the Journal of Environmental Engineering and Landscape Management. This article describes the modeling of a flow-through bioreactor with PI control. The constructed mathematical model introduces the nonlocal condition with PI controller. The author contributed to this work by participating in the mathematical model and numerical algorithm formulation process, programming of the numerical algorithms, performing numerical experiments, and making a contribution to charts and manuscript text.

In October 25-27, 2017, the author attended a conference "NSCM 30: the 30th Nordic seminar on computational mechanics" in Denmark and presented a report "PID-controlled flow-through bioreactor". The author prepared and made an oral presentation of the work in the conference.

In January 22-25, 2018, the author attended a conference (symposium) "3rd NESUS Winter School and PhD Symposium 2018" in Croatia and read a report "PID-controlled drug delivery system subject to flow-through bioreactor". The author prepared and made an oral presentation of the work in the conference.

In 2017 and 2020, the author attended a "Conference of Young Scientists" hosted by The Lithuanian Academy of Sciences in Vilnius and presented reports on bioreactor mathematical modeling subject to nonlocal and nonlocal boundary conditions. Both reports were evaluated by the committee and awarded. The author prepared and made an oral presentation of the work in the conference.

Structure of the thesis

The thesis is divided into five chapters, followed by a bibliography. The first chapter is an introduction and four subsequent chapters present the research. The summaries of four chapters are provided below.

Chapter 1

The study of a system of two parabolic nonlinear reaction–diffusion equations subject to a nonlocal boundary condition is explained. This system of nonlinear equations is used for mathematical modeling of biosensors and bioreactors. The integral type nonlocal boundary condition links the solution on the system boundary to the integral of the solution within the system inner range. This integral plays an important role in the nonlocal boundary condition and

in the general formulation of the boundary value problem. The solution at boundary points is calculated using the integral combined with the proportional-integral-derivative controller algorithm. The mathematical model was applied for the modeling and control of drug delivery systems when a prodrug is converted into an active form in the enzyme containing bioreactor before delivering into the body. The linear, exponential, and stepwise protocols of drug delivery were investigated, and the corresponding mathematical models for the prodrug delivery were created.

Chapter 2

A mathematical model for drug delivery monitoring subject to flow-through bioreactor is analyzed. The convection–diffusion–reaction model combined with PID control is used. The enzyme-containing bioreactor converts a prodrug into an active drug. This approach connects two aspects of drug delivery, mechanical pumps and prodrugs. Drug delivery monitoring is performed by adjusting the prodrug inflow pressure. Several dynamic treatment regimes are modeled. A combined algorithm of treatment regimes can be used for personalized treatment. A control-aided system allows us to reduce the impact of pumping fluctuations, diffusion slowdown, and drug production rate reduction.

Chapter 3

A mathematical model of nitrate removal in a woodchip denitrification bioreactor based on the field experiments is proposed. The inverse problem for the nonlinear system of differential convection-reaction equations is applied to optimize the efficiency of nitrate removal when changing the length of the bioreactor and flow rate. A mathematical algorithm containing a nonlocal condition represents a PI controller to monitor a flow rate when the nitrate concentration in the inflow water varies over time. Linear regression formulas are obtained for the average nitrate removal rate and the average oxygen decline rate, as well as for the rates of chemical reactions of the denitrification process with respect to temperature and pH.

Chapter 4

The stability of difference scheme for reaction-diffusion equation system was analyzed. Eigenvalue spectrum analysis for control and equation system parameters was carried out. Sufficient conditions for numerical algorithm difference scheme stability were obtained. Integral control ("I" component from

the PID controller) was introduced as a part of the nonlocal boundary condition. The essential feature of this problem is that a nonlocal boundary condition is formulated for a system of equations. The mathematical model is distinguished by a nonlocal boundary condition binding both derivatives with regard to time and space.

1. Reaction–diffusion equation with nonlocal boundary condition subject to PID-controlled bioreactor

Introduction

This chapter is based on the article [41]. This mathematical model belongs to an intensely studied class of problems, namely differential equations subject to nonlocal boundary conditions. Nonlocal boundary conditions are commonly referred to as the boundary conditions describing the relationship between the desired solution values on multiple points. Unlike classical boundary conditions, nonlocal conditions do not describe the values of the solution or its derivative in a particular range of the single boundary point. The expressions describing the nonlocal boundary conditions may contain integral expressions of the desired solution, as is the case with our model. This is commonly called a problem with nonlocal integral conditions.

Historically, the oldest mathematical works on the nonlocal conditions appear to be the book [86] and the article [71]. Here these conditions are known as the *more general boundary conditions* [92]. These works, however, have not attracted much attention. As far as the author knows, the first mathematical models with nonlocal conditions describing real physical processes appeared in scientific journals in the 1960s [11, 45]. These works, although not immediately, have attracted more consideration in scientific publications, especially in mathematical journals.

A relatively large number of mathematical models with nonlocal conditions describing real processes in a number of applications have been created over the last few decades. Among notable applications, there are heat conduction, thermoelasticity, hydrodynamics, semiconductor devices, ecology, geophysical flows, population dynamics, electrochemistry, and biotechnology (see [14, 24, 25, 44, 62, 85] and the references therein).

The main peculiarity of the present work is a sufficiently detailed explanation of the physical principles that were the basis of the nonlocal boundary condition, which reflects the control (regulation) principle. The described control system is based on four mechanisms: the given control function (set-point function), the monitoring signal (integral value, measured process variable), the control signal (computed by the PID controller), and a mechanical device providing the boundary value.

In this chapter, a system of two parabolic nonlinear reaction–diffusion equations subject to a nonlocal boundary condition is studied. Such system of nonlinear equations is used for mathematical modeling of biosensors and bioreactors [6].

The main purpose of this chapter is to provide a mathematical model suitable for the monitoring of the product molar flow into the body. To this end, a control system is used to monitor the outflow of a bioreactor through manipulation of its input parameters.

This model not only provides a set of diffusion–reaction equations, but also describes the underlying physical process together with its possible applications.

Today about 5–10% of newly introduced drugs are prodrugs [74, 93]. They are more stable and sometimes possess special parameters necessary for the treatment [93]. In the body, or even in the cell, they are converted into an active form. Very often, enzymatic conversion of a prodrug to an active form is applied. For these purposes, enzymatic capacity of the body is explored [93].

However, this approach has some limitations. There is a limited number of suitable enzymatic systems in the body and/or too low enzymatic activity. Also, there is a problem with side products of the enzymatic conversion of the prodrug into an active form. Sometimes, side products are toxic or causing undesirable effects in the body.

In some cases, before delivering the drug into the body, a prodrug outside the body should be activated. Immobilized enzyme-containing flow-through reactors can be used in this case, the prodrug on the inlet of the reactor and an active form on the outlet.

Such construction has numerous advantages. Any enzymatic system possessing suitable specificity and necessary activity can be organized inside the reactor. A polyenzymatic system capable of consuming the side products and converting them into safe products, or simply locking them within the reactor can be organized. However, enzyme-containing reactors are not very stable due to inactivation of an immobilized enzyme. Enzyme-containing reactors possess

different activities due to the variability of the conditions of the production technology. Each reactor must be calibrated before the installation and should be controlled during the whole cycle of operation. The performance of such bioreactors can be monitored by controlling the concentration of the active drug at the output of the reactor. Based on these data, the concentration of the prodrug can be monitored to achieve the necessary level of the active drug on the exit or necessary dynamics of the drug to be delivered into the body. However, this is not always possible. Sometimes, the active drug at the output cannot be detected by suitable instruments because the drug is immediately consumed or diffused. In some cases, it is possible to control the enzymatic process inside the bioreactor. For example, the hydrolysis process is led by the production of ions. This means that the conductivity of such media is increasing. Sometimes, side products of hydrolysis (or oxidation) are electrochemically active and can be easily detected. For this purpose, it is necessary to construct an analytic system inside the biochemical reactor.

The chapter is divided into sections. In Section 1.2, the model with PID control is described, and an introspection into related models is provided in Section 1.3. In Section 1.4, the process in the bioreactor is described. Section 1.5 contains the numerical results illustrated by charts and descriptions.

Mathematical model

The mathematical model consists of a system of two differential equations widely used in mathematical modeling [6]. The key feature of this model is the nonlocal boundary condition that combines two different components of the solution.

The boundary value problem is considered for the system of two nonlinear diffusion–reaction equations

$$\begin{aligned} \frac{\partial S}{\partial t} &= \mathscr{D}_S \frac{\partial^2 S}{\partial x^2} - \frac{V_{max} S}{K_M + S}, \\ \frac{\partial P}{\partial t} &= \mathscr{D}_P \frac{\partial^2 P}{\partial x^2} + \frac{V_{max} S}{K_M + S}, \end{aligned} \tag{1.1}$$

$$(x,t) \in D = \{0 < x < d, 0 < t \leq T\}, \tag{1.2}$$

with initial conditions

$$S(x,0) = \begin{cases} 0, & 0 \le x < d, \\ S_0, & x = d, \end{cases} \qquad P(x,0) = 0, \quad 0 \le x \le d, \tag{1.3}$$

and boundary conditions

$$\begin{gathered} P(0,t) = 0, \quad 0 < t \le T; \qquad \left.\frac{\partial P}{\partial x}\right|_{x=d} = 0, \quad 0 < t \le T; \\ \left.\frac{\partial S}{\partial x}\right|_{x=0} = 0, \quad 0 < t \le T. \end{gathered} \tag{1.4}$$

The last nonlocal boundary condition represents the PID control algorithm

$$S(d,t) = \mathscr{K}_p e(t) + \mathscr{K}_i \int_0^t e(\tau)d\tau + \mathscr{K}_d \frac{de(t)}{dt}, \quad 0 < t \le T. \tag{1.5}$$

The control system has two major components, the process and the controller. The process has one input, the manipulated variable (MV), also called the control variable [4]. It is denoted by $S(d,t)$. The control variable influences the process via the change of substrate concentration on the input boundary. The process output is called the process variable (PV) and is denoted by $\frac{2\mathscr{D}_p}{m^2-n^2}\int_n^m P(x,t)dx$. This variable is measured by a sensor. The desired value of the process variable is called the set-point (SP) or the reference value [4]. It is denoted by $Q(t)$. The control error $e(t)$ is the difference between the set-point and the process variable [4].

The error function $e(t)$ defines the difference between the required product molar flow $Q(t)$ and the measured flow

$$e(t) = Q(t) - \frac{2\mathscr{D}_p}{m^2-n^2}\int_n^m P(x,t)dx, \quad 0 < m,n < d, \tag{1.6}$$

$Q(t)$ is a given function (set-point), and $\mathscr{K}_p$, $\mathscr{K}_i$, and $\mathscr{K}_d$ are non-negative coefficients for the proportional, integral, and derivative terms.

If the feedback works well, the error will be small, and, ideally, it will be zero. When the error is small, the process variable is also close to the set-point irrespective of the properties of the process. To realize feedback, it is necessary to have appropriate sensors and actuators and a mechanism that performs the control actions [4].

The nonlocal boundary condition (1.5) links the value of $S(x,t)$ on the boundary where $x = d$ to the integral value of $P(x,t)$ in the inner range $[n,m]$.

The main peculiarity of the boundary condition (1.5) is its nonlocality due to the integration not only in the space domain $[n,m]$, but also in the time domain $[0,t]$. The PID controller continuously evaluates the error value $e(t)$ and attempts to minimize the error over time by adjusting the control variable $S(d,t)$ to a new value determined by (1.5).

The problem of maintaining the molar outflow of a drug (product), which may vary over time, is analyzed. It is worth noting that the properties of the physical process prohibit direct measurements at the boundary of the bioreactor; therefore, the viable options are to regulate either the concentration or the flow of the substrate (or both). In the present work, the substrate concentration is regulated.

Numerical scheme

The numerical scheme is based on the finite difference method on a uniform mesh. The space (x) is divided into equal intervals h. The time domain is divided into equal intervals τ with strict convergence condition by Courant–Friedrichs–Lewy constraint. In this particular case, $\frac{max(\mathscr{D}_S,\mathscr{D}_P)\tau}{h^2} < \frac{1}{6}$ and $\frac{V_{max}}{K_M} < \frac{1}{2}$ were applied, due to the nonlinear equations.

$$\frac{\overline{S}_i - S_i}{\tau} = \mathscr{D}_S \frac{S_{i-1} - 2S_i + S_{i+1}}{h^2} - \frac{V_{max} S_i}{K_M + S_i}, \quad 0 < i < N,$$
$$\frac{\overline{P}_i - P_i}{\tau} = \mathscr{D}_P \frac{P_{i-1} - 2P_i + P_{i+1}}{h^2} + \frac{V_{max} P_i}{K_M + P_i}, \quad 0 < i < N.$$

Initial conditions ($t = 0$):

$$S_i = \begin{cases} 0, & 0 \le i < N; \\ \widetilde{S}_0, & i = N; \end{cases} \qquad P_i = 0, \quad 0 \le i \le N.$$

Boundary conditions:

$$\overline{S}_0 = \frac{4S_1 - S_2}{3}, \quad \overline{P}_0 = 0, \quad \overline{P}_N = \frac{4P_{N-1} - P_{N-2}}{3}.$$

The Simpson's rule uses a quadratic polynomial on each sub-interval of the range $[n,m]$ to approximate the function $P(x,t)$ and to compute the definite

integral. A left Riemann sum is used to compute the definite integral from time 0 to the current time step at t of a function $e(t)$.

$$e(t) = Q(t) - \frac{2\mathscr{D}_p}{m^2 - n^2}\left[\frac{\Delta x}{3}\sum_{j=1}^{M/2}\left(P(x_{2j-2},t) + 4P(x_{2j-1},t) + P(x_{2j},t)\right)\right];$$

$$\overline{S}_N = \mathscr{K}_p e(t) + \mathscr{K}_i\left[\tau\sum_{k=0}^{R} e(k\tau)\right] + \mathscr{K}_d\left(\frac{e(t) - e(t-\tau)}{\tau}\right).$$

Here M is an even number of sub-intervals of $[n,m]$, $\Delta x = (m-n)/M$ and $x_j = n + j\Delta x$. R is the number of intervals of $[0,t]$ with constant time increment τ, current time $t = T\tau$.

Analysis of mathematical models with nonlocal boundary conditions

In this section, a number of important properties of the mathematical model (1.2)–(1.5) are provided. A comprehensive examination of how the nonlocal condition (1.5) differs from those of other authors is provided. Also, analysis and numerical solution methods for the boundary value problems with nonlocal conditions are briefly pointed out.

First of all, notice that in the boundary value problem, the value of $S(d,t)$ is not given; instead, the condition (1.5) is stated.

Several other mathematical models subject to nonlocal conditions link the solution within the range boundaries to the integral across the entire range. A typical example is given in [24], where the author describes the quasi-static flexure of a thermoelastic rod. In this case, the entropy $\eta(x,t)$ satisfies the equation

$$\left(C + \theta_0\frac{B^2}{A}\right)\frac{\partial\eta}{\partial t} = k\frac{\partial^2\eta}{\partial x^2}$$

and two nonlocal boundary integral conditions

$$\eta(-l,t) = \frac{\theta_0 B^2}{2cAl^2}\int_{-l}^{l}(l-3x)\eta(x,t)dx,$$

$$\eta(l,t) = \frac{\theta_0 B^2}{2cAl^2}\int_{-l}^{l}(l+3x)\eta(x,t)dx$$

In many articles [14, 32, 44], the authors study mathematical models subject to nonlocal conditions that include the solution or its derivative values only over the boundary points. In the one-dimensional case, there are only two points, the endpoints of the interval. Various nonlocal conditions based only on the values of the solution at the endpoints are rather widely analyzed in numerical analysis, peculiarly w.r.t. the stability of difference schemes (see [32] and references therein).

All the previously discussed mathematical models with nonlocal conditions are defined by a single second-order differential equation. The mathematical model (1.2)–(1.5) is defined as a system of two differential equations with a nonlocal condition (1.5), which links the solutions of the equations $S(d,t)$ and $P(x,t)$. One of the first mathematical models that considers a system of two differential equations subject to nonlocal conditions was published in the monograph [83], where the mathematical models that describe the processes occurring in bioreactors are studied. Bioengineers widely use the mathematical model of an ideal reactor, the purpose of which is prediction of changes in the considered system.

The processes occurring in the bioreactors are defined as a system of two differential equations (1.2), which are similar to the equations considered in the present study but are subject to a different kind of nonlocal conditions (1.5). The conditions stated in [83] are defined only at the boundary points.

Let's point out another peculiarity of the model (1.2)–(1.5). It is worth noting that the goal is not to simply solve the problem (1.2)–(1.5) once with given parameter values. Instead, the focus is to pick the boundary substrate concentration $S(d,t)$ in such a way that the product value $P(x,t)$ would possess a specific property defined beforehand. In the simplest case, the aim is to obtain the value of $S(d,t)$ that minimizes the absolute value of $e(t)$.

In this sense, the mathematical model (1.2)–(1.5) is similar to (but does not fully match) the inverse problem with the overdetermination (observation) condition.

The class of inverse problems is closely related to the issue of control. Namely, the nonlocal (typically, integral) condition is used together with, and not instead of, the boundary or initial conditions. This extra condition is usually termed as the overdetermination (or observation) condition. The reasoning behind the use of such condition is the necessity of finding not only the solution itself, but also an unknown function of the equation, typically interpreted as a characteristic of the energy source. An example of this can be found in [46].

Another example [91] concerns the situation where the overdetermination condition is not a boundary condition, but instead is the value of the final solution. In this case, it is required to solve a second-order parabolic equation with the usual boundary conditions and, in addition, the final overdetermination condition. This additional condition means that the value of the solution at time T must coincide with the given function, and hence the equation contains this unknown function (a characteristic of the source). The physical interpretation of this problem is related to the issue of the environmental safeguard in densely populated cities [91]. For comparison purposes, it is worth noting that in this case the overdetermination condition takes a more complicated form and requires a particularly fine minimization of $e(t)$.

Yet another trait of the model (1.2)–(1.5) is that the nonlocality in clause (1.5) in the general case is twofold: first, w.r.t. the spatial variable x and, second, w.r.t. the time t. These two types of nonlocality are different, and, as far as the author knows, both have not been jointly addressed in the references.

The spectrum of the differential operator plays an important role in the stability of the numerical solutions of simpler mathematical models with nonlocal conditions [32, 39, 40, 43, 44, 77]. Note that the parameter values of the nonlocal condition can significantly change the structure of the spectrum. Therefore, the theoretical study of the considered mathematical model (1.2)–(1.5) subject to the double integral is an important task and poses new challenges for numerical experiments.

As a final remark, the mathematical models with nonlocal conditions describing real physical processes have been strongly encouraging the theoretical studies of differential equations and numerical methods.

Many authors who considered the problems subject to nonlocal conditions emphasized that the nonlocal boundary value problems have certainly been one of the most rapidly growing areas in various application fields. Hence, the development of numerical methods for solving the nonlocal boundary value problems has also been an important research area. The author agrees with these statements, but also prefers to rephrase them. The progress made in the study of numerical methods subject to nonlocal boundary value problems is indeed significant. However, there is still not enough feedback from the numerical methods studies toward practical applications. Too few works are devoted to the study of the new effects in application areas subject to nonlocal boundary value problems. Such effects cannot be identified using the normal classical conditions. Therefore, by the present chapter the author tries to strengthen the

feedback effect of the mathematical models with nonlocal conditions.

Physical model

The enzymatic reaction is considered

$$S \xrightarrow{Enzyme} P,$$

where S is a substrate of the enzyme considered as a prodrug, and P is one of the products of the enzymatic reaction to be controlled and considered as the active drug (or the side product). The expected concentration of the side product correlates with the concentration of the active drug. Therefore, P is considered as the concentration of the active drug, which can be monitored by an independent method (usually, electrochemical and sometimes optical). The enzymatic conversion of the substrate can be derived as the Michaelis–Menten process:

$$V_P = \frac{V_{max} S}{K_M + S},$$

where V_P is the product generation rate at a particular point within the bioreactor.

Table 1.1: Model constants and properties

S	$\mathrm{mol} \cdot \mathrm{m}^{-3}$	moment substrate concentration at the same particular point of the bioreactor
P	$\mathrm{mol} \cdot \mathrm{m}^{-3}$	moment product concentration at the same particular point of the bioreactor
S_0	$0\ \mathrm{mol} \cdot m^{-3}$	initial substrate concentration
V_{max}	$1.1 \times 10^{-3}\ \mathrm{mol} \cdot \mathrm{m}^{-3} \cdot \mathrm{s}^{-1}$	maximum reaction speed (maximal activity of the enzyme)
K_M	$2 \times 10^{-1}\ \mathrm{mol} \cdot \mathrm{m}^{-3}$	Michaelis constant typical for such substrate and such enzyme
$\mathscr{D}_S$	$5 \times 10^{-6}\ \mathrm{m}^2 \cdot \mathrm{s}^{-1}$	diffusion coefficient of substrate
$\mathscr{D}_P$	$5 \times 10^{-6}\ \mathrm{m}^2 \cdot \mathrm{s}^{-1}$	diffusion coefficient of product
d	$1 \times 10^{-3}\ \mathrm{m}$	bioreactor thickness
$[n;m]$	$[1;2] \times 10^{-4}\ \mathrm{m}$	measuring range
t	s	time
T	s	reaction duration

Suppose that an enzyme is immobilized in a drug delivery system named

as a bioreactor (Fig. 1.1). The enzyme is uniformly distributed in the bioreactor. The bioreactor containing the immobilized enzyme is permeable for the substrate, which means that the substrate S can diffuse in the bioreactor with diffusion coefficient $\mathscr{D}_S$. When substrate molecules reach the active center of the immobilized enzyme, the substrate is converted into the product P at the rate V_p. The product P diffuses inside the bioreactor with diffusion coefficient $\mathscr{D}_P$. The initial ($t = 0$) concentration of the product P at the inlet (d) boundary of the bioreactor is set to zero ($P(d,0) = 0$). Inside the bioreactor, an electrode wire net (electrode) is deposited in order to perform the electrochemical monitoring of the enzymatic reaction. On the outer surface of the bioreactor, a reservoir with adjustable concentration of the substrate is deposited. Let's consider that the concentration of the substrate S can be monitored depending on the response of the electrochemical electrode.

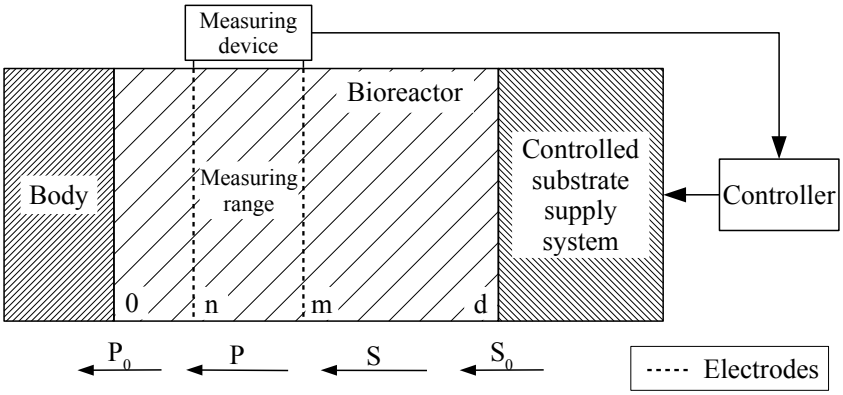

Figure 1.1: Principal structure of bioreactor

The given bioreactor can be represented as an active transdermal patch. The transdermal patch is applied to the patient's skin; one side of the transdermal patch delivers the drug (product) to the patient, whereas the other side is equipped with a controlled substrate (prodrug) supply system, which is designed to alter the substrate concentration or its flow. The transdermal patch is equipped with two electrodes that measure the electrochemical characteristics of the specific drug. In this way, it controls the concentration of the drug in the inner range of the transdermal patch.

The treatment process requires the drug to be transferred to a patient in accordance with the therapeutic protocol. This can be either a constant flow or a function of the time, for example, in the early treatment stage the drug flow

must start at a high value and then gradually decline as the treatment progresses, or the drug dose must continually rise until reaching a prescribed value.

Results

Depending on the disease and the patient's medical condition, a specific treatment protocol should be applied. During the treatment process, the patient must receive a strictly prescribed drug dose. Three treatment protocols are provided: linear, exponential, and stepwise.

A numerical modeling was performed using a computer program developed by the author. It implements an explicit finite difference scheme using a forward difference at time and a second-order central difference for the space derivative. The integral was computed by the Simpson's rule. The computed values of a substrate were used as an input for the product value computation at the next step. The model properties are defined in Table 1.1, and all the additional properties are presented later in the text.

The control algorithm was applied to three treatment protocols, which are presented by different functions $Q(t)$. The results of the linear treatment protocol modeling are shown in Fig. 1.2, where $Q(t)$ is a linear function.

In Fig. 1.2, it is shown how the PID controller performs over the set-point function $Q(t)$, which was set to the linear treatment protocol mode. In the beginning of the process, the substrate concentration in the reactor is zero, and the value of the error function is high; therefore, the observed substrate concentration from the beginning up to half a second is relatively high, whereas the flow of the product is rising until it reaches the set-point. Also, a little product flow overshoot and a slight drop until it reaches the required level set by the set-point function is shown. Later, while the product flow value is close to the set-point, the monotonous decrease in substrate concentration is observed.

The second treatment protocol uses the exponential function $Q(t)$. Basically, the exponential treatment protocol (Fig. 1.3) differs from the linear one only in the derivative of the set-point function, which is changing over time. Initially, the absolute value of the derivative is larger, but over time it decreases. From the beginning of the process, an overshoot of the product flow is observed, which is reduced later on. The smaller the absolute value of the derivative of the set-point function, the quicker the stabilization of the control mechanism. Accordingly, for this short (3 seconds) treatment process, it is more difficult to

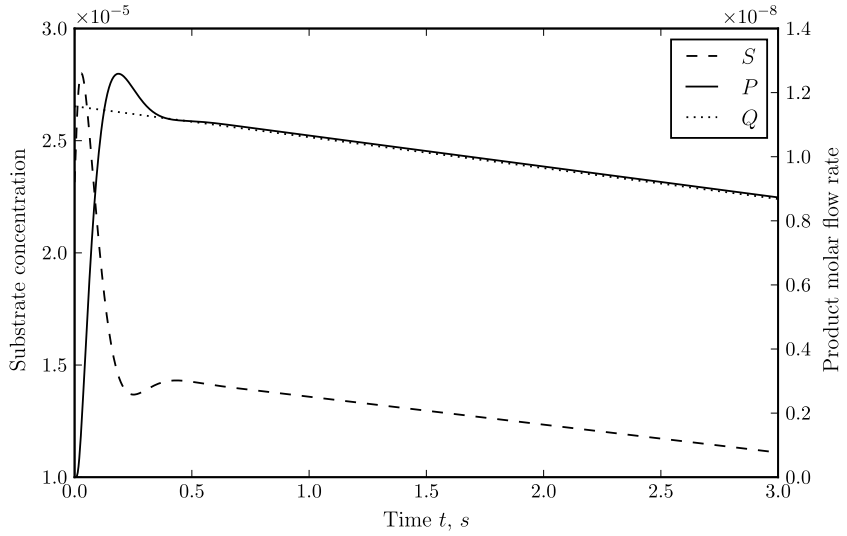

Figure 1.2: Linear treatment protocol. Substrate (S) concentration $S(d,t)$, $mol \cdot m^{-3}$, left axis. Product (P) molar flow rate $\mathscr{D}_p \frac{\partial P}{\partial x}\Big|_{x=0}$ and set-point function $Q(t)$, $mol \cdot m^{-2} \cdot s^{-1}$, right axis. Parameters $\mathscr{K}_p = 2000, \mathscr{K}_i = 25000, \mathscr{K}_d = 80000$.

stabilize in the beginning.

The third protocol uses the stepwise function $Q(t)$. The peculiarity of this protocol is that the drug flow over time decreases in steps and the required drug flow value is a piecewise constant function.

The stepwise treatment protocol (Fig. 1.4) is different from both the linear and exponential ones. In this case, the set-point function $Q(t)$ is discontinuous. The PID control algorithm with experimentally selected values of the parameters ($\mathscr{K}_p$, $\mathscr{K}_i$, $\mathscr{K}_d$) is able to control the process of this kind. As long as the product flow has not reached the set-point value, the control process is similar to the linear or exponential ones. Later on, the controller adjusts the substrate concentration, which in turn stabilizes the product flow. When the set-point function value changes, the substrate concentration should be adjusted accordingly. Starting from the 2nd second, a rapid decrease of the substrate concentration is seen, which then increases again until stabilization.

In this case, a short-time treatment process (only 3 seconds) is modeled, whereas the real treatment process requires considerably more time.

These examples visually demonstrate the control mechanism and its ability to satisfy the requirements for a variety of treatment protocols (represented as

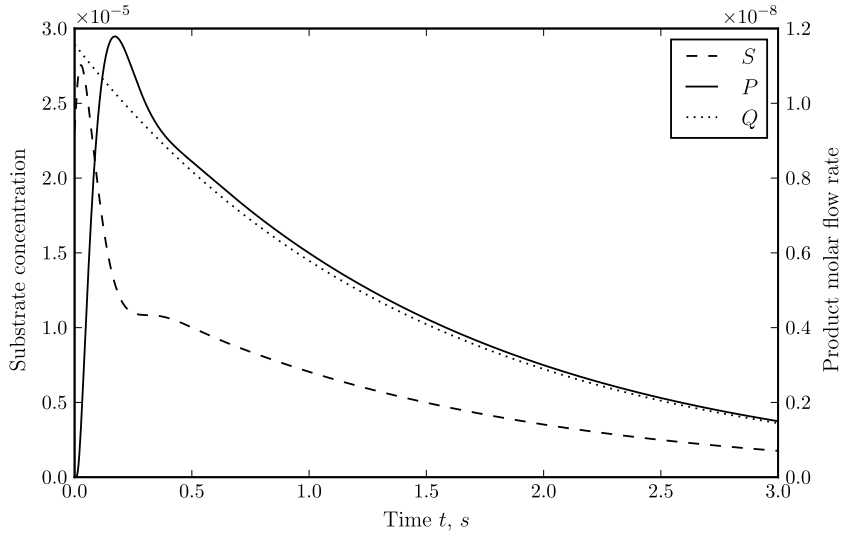

Figure 1.3: Exponential treatment protocol. Substrate (S) concentration $S(d,t)$, $mol \cdot m^{-3}$, left axis. Product (P) molar flow rate $\mathscr{D}_p \frac{\partial P}{\partial x}\Big|_{x=0}$ and set-point function $Q(t)$, $mol \cdot m^{-2} \cdot s^{-1}$, right axis. Parameters $\mathscr{K}_p = 2000, \mathscr{K}_i = 25000, \mathscr{K}_d = 80000$.

different set-point functions $Q(t)$). During this short modeling time, the control mechanism is able to stabilize and maintain a complex process. A numerical study revealed that long running treatment processes can apply the existing model, as the critical actions were maintained at the short periods of time (see Fig. 1.4, time 0–0.5 s and 2–2.5 s).

Conclusions

In this chapter, a new type of nonlocal boundary condition for the parabolic reaction–diffusion equation system applied to the bioreactor modeling is proposed. The condition is nonlocal w.r.t. the time and space domains.

The double integral of this type in the nonlocal condition poses new challenges for numerical experiments related to this mathematical model. The spectrum of the differential operator plays an important role in the stability of the numerical solutions of simpler mathematical models with nonlocal conditions. The parameter values of the nonlocal condition can significantly change the structure of the spectrum. Therefore, the theoretical study of the considered

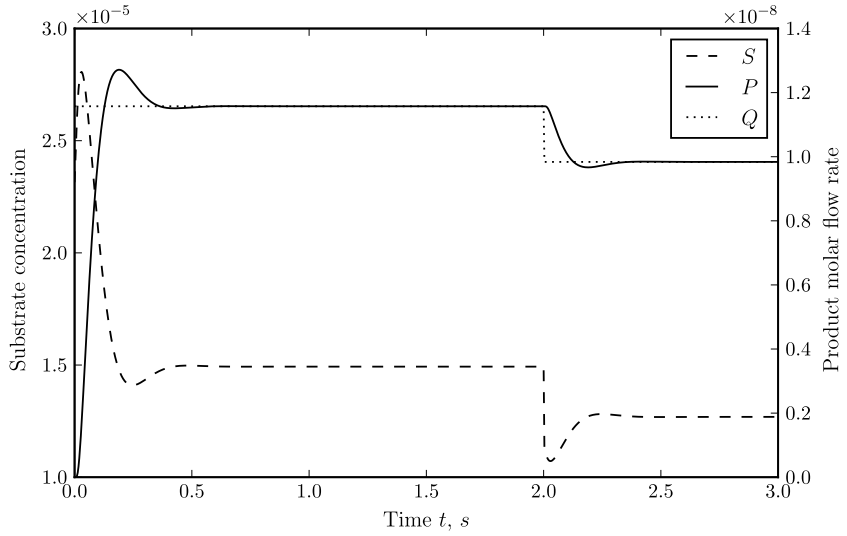

Figure 1.4: Stepwise treatment protocol. Substrate (S) concentration $S(d,t)$, $mol \cdot m^{-3}$, left axis. Product (P) molar flow rate $\mathscr{D}_p \frac{\partial P}{\partial x}\Big|_{x=0}$ and set-point function $Q(t)$, $mol \cdot m^{-2} \cdot s^{-1}$, right axis. Parameters $\mathscr{K}_p = 2000, \mathscr{K}_i = 25000, \mathscr{K}_d = 80000$.

mathematical model is an important task.

The mathematical model was applied to the modeling operation and control of drug delivery systems when the prodrug is converted into an active form in the enzyme-containing bioreactor before being delivered into the body. The linear, exponential, and stepwise protocols of drug delivery were investigated, and the corresponding mathematical models for the prodrug delivery were created.

2. Drug delivery mathematical modeling for pressure controlled bioreactor

Introduction

This chapter is based on the article [54]. Controlled drug delivery systems has been a hot topic of the pharmacy and pharmacokinetics for several decades. In general, drug delivery systems can be divided into two main directions: mechanical pumps and prodrugs. A number of programmed drug delivery pumps (like insulin pumps) were designed and implemented.

Drug delivery systems can have a wide variety of parameters to be tuned. Having the requirements set for a particular system, a mathematical model can be used to fine-tune these parameters and provide only the matching ones. Great attention was paid to the mathematical modeling of the drug delivery systems and control of their action. Various drug delivery aspects were discussed and reviewed [68, 70, 84].

A lot of prodrugs exist in nature and can be extracted from plants, microorganisms, animal and marine sources [52]. A number of modifying agents can be used in prodrugs. Some of them are suitable transporters [1, 64]. An amino acid transporter usually facilitates penetration of the prodrug through skin [27, 66]. There are a number of other transporters: bile acid, carnitine, glucose, peptide, vitamin C, multivitamin, etc.

Some drugs are not stable. For instance, to improve the stability and solubility of bufalin, a number of chemical modifiers were applied [61]. The majority of prodrugs are converted into an active form inside the body. In this case, the body enzymatic systems are used. Hence, this approach has some limitations. In the body there are limited number of suitable enzymatic systems. Also, there is a problem with side products: they can be toxic or may cause undesirable effects.

This chapter describes theoretical considerations of the prodrug conversion into the active form directly before injection of the drug. The control aided sys-

tem subject to the convection–diffusion–reaction bioreactor for the conversion of the prodrug to the active form, i.e. drug, is considered. Released stabilizing chemical groups of the prodrug should be locked inside the reactor, thus only the active form of the drug will be injected into the body.

Such bioreactor is a part of the drug delivery system. The particular approach binds both aspects of drug delivery: mechanical pumps and prodrugs.

However, the biocatalytic activity of a column (bioreactor) is varying, for example, due to inactivation of immobilized enzyme, inhibition or gluing and etc. A sensing system is installed in the column to monitor prodrug conversion level and rate. This device can be designed to measure the outflow of the drug to control the drug supply system.

A controlled injection of the drug will allow to implement different regimes of the drug delivery. The present model was used to simulate the control of three different therapeutic drug delivery regimes.

The given model can be applied in precision medicine (personalized medicine). Monitored treatment systems can reduce human error and allow to design them to be more reliable and effective.

Physical model

Let's consider an unstable drug attached to the stabilizing agent (block). Such derivative (drug-block) is pumped through the bioreactor (column) with the immobilized enzyme, where the block is being removed and the drug is being released.

$$DRUG - BLOCK \xrightarrow{ENZYME} DRUG + BLOCK$$

A number of enzymes can catalyze the conversion of a prodrug into an active drug. Let's consider the activation of the drug by hydrolysis of the prodrug. The block should be trapped inside the bioreactor. Thus, only the active drug will be delivered into the body. Another approach is the bioreactor with the immobilized enzyme and additionally attached trapping filter to capture the block.

In both cases, some conditions should be applied. Firstly, the prodrug should be fully converted into an active form. Secondly, the block should be completely trapped inside the column. Only in some cases, when the block

is not toxic, trapping of the side products of the enzymatic reaction is not necessary (for example, glycosylated form of the drug).

For clarity, the prodrug (drug-block) will be denoted as S (substrate for the enzyme), and the active form of the drug - P (product of enzymatic reaction).

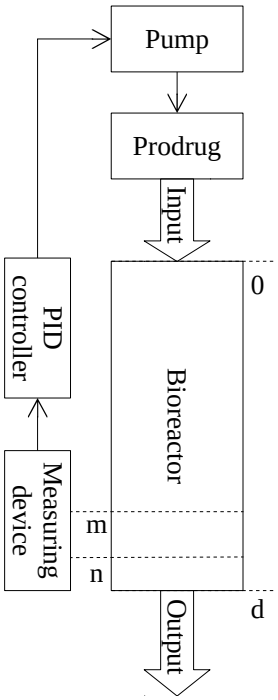

Figure 2.1: Principal structure of bioreactor

The enzyme is uniformly distributed inside the bioreactor. The column containing the immobilized enzyme is permeable to the substrate S. It can diffuse within the bioreactor with diffusion coefficient $\mathscr{D}_S$. When the additional inflow pressure is applied, the flow of the substrate and product consists of diffusion and pressure-based (convection) flows.

When substrate molecules reach the active center of the immobilized enzyme, the substrate is converted into the product P at the rate V_p. The product P diffuses inside the bioreactor with diffusion coefficient $\mathscr{D}_P$.

The concentration of the product P on the boundary of the bioreactor is given by P_0. Inside the bioreactor, an electrode wire net (electrode) is placed in order to perform the electrochemical monitoring of the enzymatic reaction. Optical sensors as well as biosensors [53] can be applied. A sensor signal is used as a measured process variable for the PID controller.

On the outer surface of the bioreactor, a reservoir with the substrate is

located. Let's consider that the flow rate of the substrate S can be adjusted by the pressure relying on the PID control [42].

The treatment process requires the drug to be transferred to a patient in accordance with the therapeutic regime. This can be either a constant flow or a time function (e.g. in the early treatment stage the drug flow must start at a high value and then gradually decline as the treatment progresses, or the drug dose must continually rise until reaching a prescribed value) [42].

Table 2.1: Model constants and properties

S	$\mathrm{mol} \cdot \mathrm{m}^{-3}$	moment substrate concentration at the same particular point of the bioreactor
P	$\mathrm{mol} \cdot \mathrm{m}^{-3}$	moment product concentration at the same particular point of the bioreactor
S_0	$2.5\ \mathrm{mol} \cdot \mathrm{m}^{-3}$	initial substrate concentration
V_{max}	$4 \times 10^{-3}\ \mathrm{mol} \cdot \mathrm{m}^{-3} \cdot \mathrm{s}^{-1}$	maximum reaction speed (maximal activity of the enzyme)
K_M	$2 \times 10^{-1}\,\mathrm{mol} \cdot \mathrm{m}^{-3}$	Michaelis constant typical for such substrate and such enzyme
$\mathscr{D}_S$	$5 \times 10^{-8}\,\mathrm{m}^2 \cdot \mathrm{s}^{-1}$	diffusion coefficient of substrate
$\mathscr{D}_P$	$5 \times 10^{-8}\,\mathrm{m}^2 \cdot \mathrm{s}^{-1}$	diffusion coefficient of product
d	$5 \times 10^{-2}\,\mathrm{m}$	bioreactor thickness
$[n;m]$	$[1;2] \times 10^{-3}\,\mathrm{m}$	measuring range
t	s	time
T	s	reaction duration

Mathematical model

In the previous chapter, the diffusion–reaction bioreactor subject to PID control was analyzed. This chapter extends a previously discussed mathematical model.

The model is defined as two convection–diffusion–reaction differential equations. The convection term represents a controlled pressure mechanism.

$$\begin{aligned}
\frac{\partial S}{\partial t} &= \mathscr{D}_S(t)\frac{\partial^2 S}{\partial x^2} + \alpha(t)\frac{\partial S}{\partial x} - \frac{V_{max}(t)S}{K_M + S}, \\
\frac{\partial P}{\partial t} &= \mathscr{D}_P(t)\frac{\partial^2 P}{\partial x^2} + \alpha(t)\frac{\partial P}{\partial x} + \frac{V_{max}(t)S}{K_M + S},
\end{aligned} \tag{2.1}$$

$$(x,t) \in D = \{0 < x < d, 0 < t \leq T\}. \tag{2.2}$$

The starting empty state of the bioreactor is defined as initial conditions

$$S(x,0) = \begin{cases} 0, & 0 \leq x < d, \\ S_0, & x = d, \end{cases} \qquad P(x,0) = 0, \quad 0 \leq x \leq d, \tag{2.3}$$

and the boundary conditions (input and output boundaries) that allow to outflow both the drug **(P)** and the prodrug **(S)** with constant prodrug **(S)** concentration on the input edge

$$\begin{aligned}
P(0,t) &= 0, \quad 0 < t \leq T, \\
P(d,t) &= 0, \quad 0 < t \leq T, \\
S(0,t) &= 0, \quad 0 < t \leq T, \\
S(d,t) &= S_0, \quad 0 < t \leq T.
\end{aligned} \tag{2.4}$$

Drug outflow is controlled via the pressure on the input edge. The pressure control system adopts a PID control loop feedback mechanism. The system monitors the drug outflow and adjusts the pressure. The key nonlocal condition defining the control system is

$$\alpha(t) = \mathscr{K}_p e(t) + \mathscr{K}_i \int_0^t e(\tau)d\tau + \mathscr{K}_d \frac{de(t)}{dt}, \quad 0 < t \leq T. \tag{2.5}$$

An error function $e(t)$ at each moment of time evaluates the difference between the required drug outflow and the actual measured one. The required drug outflow is set by $Q(t)$, a given set-point function.

$$e(t) = Q(t) - \frac{2\mathscr{D}_p}{m^2 - n^2} \int_n^m P(x,t)dx, \quad 0 < m,n < d. \tag{2.6}$$

The PID controller continuously evaluates an error value $e(t)$ and attempts to minimize it over time by adjusting the control variable (pressure) α to a new value determined by (2.5).

$\mathscr{K}_p$, $\mathscr{K}_i$, and $\mathscr{K}_d$ are non-negative coefficients for the proportional, integral, and derivative terms in a PID scheme. They are used to set a regime of the controller, and by tuning these coefficients the controller function can be changed to respond quicker or slower, with more or less overshoot.

Numerical scheme

A numerical scheme is based on the finite difference method on a uniform mesh. The space (x) is divided into equal intervals h. The time domain is divided into equal intervals τ with strict convergence condition by Courant–Friedrichs–Lewy constraint. In this particular case, $\frac{max(\mathscr{D}_S,\mathscr{D}_P)\tau}{h^2} < \frac{1}{6}$, $\frac{V_{max}}{K_M} < \frac{1}{2}$ and $\frac{\alpha(t)}{h} < \frac{1}{4}$ were applied.

$$\frac{\overline{S}_i - S_i}{\tau} = \mathscr{D}_S(t)\frac{S_{i-1} - 2S_i + S_{i+1}}{h^2} + \alpha(t)\frac{S_{i+1} - S_{i-1}}{2h} - \frac{V_{max}S_i}{K_M + S_i};$$
$$\frac{\overline{P}_i - P_i}{\tau} = \mathscr{D}_P(t)\frac{P_{i-1} - 2P_i + P_{i+1}}{h^2} + \alpha(t)\frac{P_{i+1} - P_{i-1}}{2h} + \frac{V_{max}P_i}{K_M + P_i}.$$

Initial conditions ($t = 0$):

$$S_i = \begin{cases} 0, & 0 \le i < N; \\ \widetilde{S}_0, & i = N; \end{cases} \qquad P_i = 0, \quad 0 \le i \le N.$$

Boundary conditions:

$$\overline{S}_0 = 0, \quad \overline{S}_N = \widetilde{S}_0, \quad \overline{P}_0 = 0, \quad \overline{P}_N = 0.$$

The Simpson's rule uses a quadratic polynomial on each sub-interval of the range $[n,m]$ to approximate the function $P(x,t)$ and to compute the definite integral. A left Riemann sum is used to compute the definite integral from time 0 to the current time step at t of a function $e(t)$.

$$e(t) = Q(t) - \frac{2\mathscr{D}_p}{m^2 - n^2}\left[\frac{\Delta x}{3}\sum_{j=1}^{M/2}\left(P(x_{2j-2},t) + 4P(x_{2j-1},t) + P(x_{2j},t)\right)\right],$$

$$\alpha(t) = \mathscr{K}_p e(t) + \mathscr{K}_i\left[\tau\sum_{k=0}^{R} e(k\tau)\right] + \mathscr{K}_d\left(\frac{e(t) - e(t-\tau)}{\tau}\right).$$

Here, M is an even number of sub-intervals of $[n,m]$, $\Delta x = (m-n)/M$ and $x_j = n + j\Delta x$. R is the number of intervals of $[0,t]$ with constant time increment τ, current time $t = T\tau$.

Numerical simulation results

A long-time treatment process (12 hours) is modeled, since the real treatment process requires approximately the same or even longer period of time. During the drug infusion action, a number of parameters can change (e.g. $\mathscr{D}_S$, $\mathscr{D}_S$, V_{max}). This chapter describes 3 major impact factors for the drug delivery system. The first one is the diffusion slowdown, the second – the drug production speed and the third is the pump impact.

Control of diffusion slowdown

During the treatment process, the diffusion of a prodrug and drug itself can be impacted by various reasons (gluing of the column with side product of the enzymatic conversion of the prodrug (BLOCK), aging of the matrix, etc.). The diffusion rate can change over time. This variating impact property is defined as diffusion functions $\mathscr{D}_S(t)$ and $\mathscr{D}_P(t)$.

The slowdown of the diffusion process was analyzed. The modeled PID controlled bioreactor is able to handle the $\mathscr{D}_S(t)$ and $\mathscr{D}_P(t)$ reduction by 19% showing the total delivered drug amount difference of 0.1%.

V_{max} variation impact

All enzyme-containing bioreactor's activity decreases in time due to the enzyme inactivation or degradation, or other reasons [88]. Therefore, the drug

outflow rate declines.

The reaction rate defined by the function $V_{max}(t)$. 10% decrease of $V_{max}(t)$ for the treatment period is modeled.

While the enzymatic reaction is slowing down, the drug production rate declines. The bioreactor outputs both the drug and the prodrug. If the reaction speed is in the range of normal operation mode, the prodrug concentration in the mixture is very low (less $1/10^4$ parts). If the prodrug outflow concentration increases, this could harm the patient. The bioreactor monitoring system will stop the process straight away, after the threshold value is reached. By modeling such an event before trials, the reliability of the system can be improved.

Within the parameters of the present bioreactor, it can handle a reduction of V_{max} by 16% giving the total delivered drug amount difference of 0.1%.

Pumping stability

Peristaltic pumps have an extensive range of uses, they are reliable and simple to maintain. However, their flow is pulsed. The pump is receiving commands to set the pressure value. Due to the recalibration or damage of a pump, it will set value with an error and the actual set value can mismatch.

In such case, the PID controller is designed to have tolerance for this kind of scenario. If the value set by the feedback mechanism fails to reach the required value, the PID controller will readjust the value, and the set-point function will be reached, no matter if the pump will set the value with an error.

A peristaltic pump with 2 s rotation period was analyzed. Within the given parameters from Table 2.1 and $\mathscr{K}_p = 2$, $\mathscr{K}_i = 10$, the bioreactor control system handles fluctuation of the pump with amplitude of 25% giving the discrepancy for delivered drug amount of 0.01%.

Treatment regimes

The dynamic treatment regime was modeled. It is a set of rules for choosing effective treatments for individual patients [56]) with several different stages.

Three different stages were combined. From the start, the step-wise regime was applied to reach the constant drug flow, the next transition (250 min.) represents the linear and the final (533 min.) represents the exponential regimes

accordingly. This configuration of treatment was chosen to test the control system with a close-to-real example.

The treatment process modeled with a set of parameters from Table 2.1 is presented in Fig. 2.2. Mathematical modeling allows to take into account the impacting factors: permeability, activity and unstable pumping.

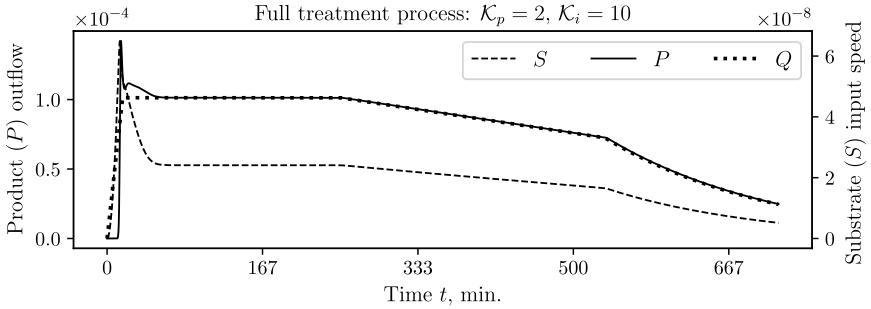

Figure 2.2: Full treatment process (12 hours). Substrate (S) input speed (m/s), right axis. Product (P) molar outflow rate $\mathscr{D}_p \frac{\partial P}{\partial x}\Big|_{x=0}$ and set-point function (Q) $Q(t)$ ($mol \cdot m^{-2} \cdot s^{-1}$), left axis. Parameters $\mathscr{K}_p$ and $\mathscr{K}_i$ present in chart subtitle, $\mathscr{K}_d = 10^5$.

To set the treatment regime, there was a need to construct a set-point function $Q(t)$. The drug outflow control will adjust the pressure to follow the required value of $Q(t)$.

A set-point function $Q(t)$ is created as follows. From the beginning, it constantly increases (0 – 16 min.) the dosage of a drug to reach the prescribed maximum and following this constant rate (16 – 250 min.). The treatment process finalization is combined of two steps: the linear decreasing stage (250 – 533 min.), followed by the exponentially declining (from 533 min.) drug dosage.

Step-wise treatment regime

In Fig. 2.3, an example of the PID control with two different sets of control equation parameters is presented. One set is representing a slightly aggressive (dynamic) mode (bottom chart) with quicker warm-up and stabilization period, while the other one (top chart) is milder and settles over an extended period of time.

From the beginning, the bioreactor is empty, no drug is being produced yet (Fig. 2.3, where P is equal to zero). After the process starts, an initial lag-period

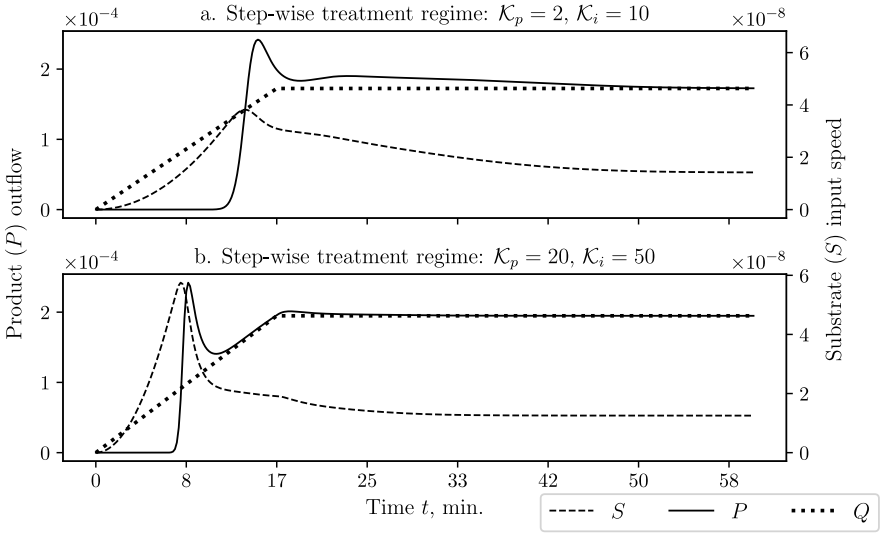

Figure 2.3: Step-wise treatment regime. Substrate (S) input speed (m/s), right axis. Product (P) molar outflow rate $\mathscr{D}_p \frac{\partial P}{\partial x}\Big|_{x=0}$ and set-point function (Q) $Q(t)$ ($mol \cdot m^{-2} \cdot s^{-1}$), left axis. Parameters $\mathscr{K}_p$ and $\mathscr{K}_i$ present in separate chart subtitles, $\mathscr{K}_d = 10^5$. Time axes are aligned.

is observed before the outflow of the drug begins (Fig. 2.3 where P rises from zero, 12 min. (top chart) 7 min. (bottom chart)).

To reduce the initial lag period (Fig. 2.3 bottom chart), one can rise the pumping rate. In this case, a sharp peak-type excess of the drug outflow will arise (Fig. 2.3, 8 min., bottom chart). If this overdose is critical for a patient, the bioreactor control can be modified to operate in a less aggressive mode (Fig. 2.3, top chart). Different control constants ($\mathscr{K}_p$, $\mathscr{K}_i$, $\mathscr{K}_d$) are used. In this case, it will have longer warm-up and stabilization periods.

In cases when the drug outflow should strictly follow the set-point function ($Q(t)$) and omit overshoot or spikes, the treatment can be started after the warm-up has ended.

Linear and exponential treatment regimes

The linear treatment regime presents the constantly declining set-point function $Q(t)$, while the rate of change declines over time in the exponential treatment regime example. The difference from the linear is the changing rate of decline. Both cases are presented in Fig. 2.4.

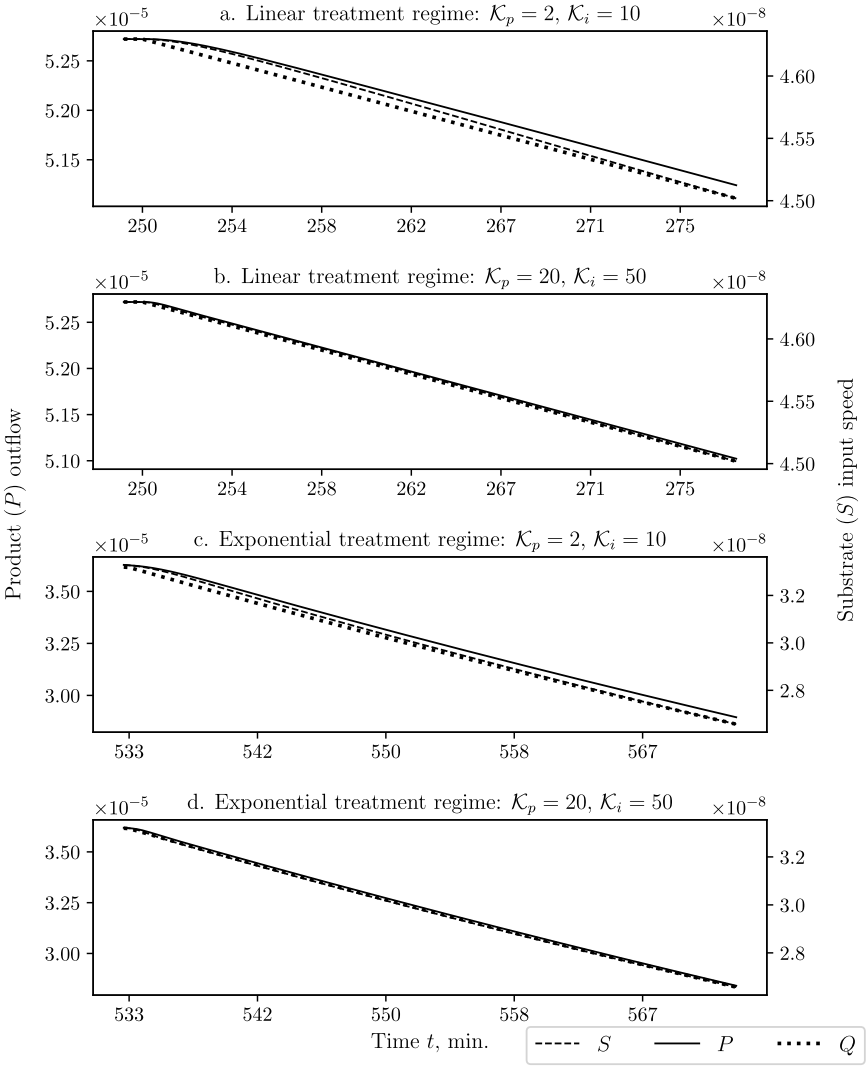

Figure 2.4: Treatment regimes. Substrate (S) input speed (m/s), right axis. Product (P) molar outflow rate $\mathscr{D}_p \frac{\partial P}{\partial x}\Big|_{x=0}$ and set-point function (Q) $Q(t)$ ($mol \cdot m^{-2} \cdot s^{-1}$), left axis. Parameters $\mathscr{K}_p$ and $\mathscr{K}_i$ present in chart subtitles, $\mathscr{K}_d = 10^5$.

Two parts from a full treatment process from Fig. 2.2 were extracted. The example charts (Fig. 2.4) show the action of control for two different ($\mathscr{K}_p = 2$, $\mathscr{K}_i = 10$) and ($\mathscr{K}_p = 20$, $\mathscr{K}_i = 50$) sets of parameters.

In both regime cases (linear and exponential), the individual divergence from the set-point function $Q(t)$ of the curves is observed. The resulting drug

outflow in the linear part of the regime diverges from $Q(t)$ by: a. 0.23%, b. 0.05%, and in the exponential example by: c. 1.01% and d. 0.20%.

Given a continuous set-point function $Q(t)$, an adequately controlled system is obtained. The results of the numerical modeling demonstrate an ability to control complicated systems. The tuning of the PID controller parameters ($\mathscr{K}_p$, $\mathscr{K}_i$ and $\mathscr{K}_d$) allows to adjust the operational mode of the bioreactor according to specific treatment process requirements.

Conclusions

The convection–diffusion–reaction model combined with PID control to monitor the drug delivery was applied. The modeled flow-through bioreactor was used to convert a prodrug into an active drug form. The control was performed by adjusting the flow rate based on the drug outflow measurements.

The PID controller allows to reduce the impact of fluctuations of pumping, diffusion slowdown and reduction of drug production rate. The ranges for reliable drug production were computed. It gives an ability to intercept the drug delivery at any moment if a malfunction is detected. Several dynamic treatment regimes were modeled and they showed the potential correct and reliable results.

The given numerical results are obtained by using a chosen set of parameters. However, the model itself allows to perform modeling with a wide spectrum of parameters and gives engineers an ability to validate their ideas numerically. Such modeling allows to optimize systems for specific requirements.

3. Mathematical modeling of nitrate removal in woodchip denitrification bioreactor

This chapter is based on the manuscript which is the result of original research submitted on June 15, 2020 and accepted on March 23, 2021 by *The Journal of Environmental Engineering and Landscape Management*.

Introduction

Release of nitrate (NO_3^-) from agricultural sources is a significant surface water quality problem occurring in many areas around the world. This problem is particularly severe in humid climates where subsurface (tile) drainage systems have been installed. The spread of fertilizers combined with agricultural drainage practices accelerates nutrient losses from the soil with subsequent development of eutrophication in receiving waters.

As a new technology, woodchip denitrification bioreactors for tile drainage are being investigated for practical edge-of-field NO_3^- removal. This technology is based on routing tile drainage water through woodchip bioreactors where nitrate is used by bacteria to oxidize carbon while reducing NO_3^- to nitrogen gas or other volatile nitrogen compounds. Microbial denitrification is recognized as a crucial mechanism governing the nitrate removal in bioreactors. Various studies have suggested that bioreactors promoting heterotrophic denitrification are low cost techniques for NO_3^- removal [18, 30, 36]. The first attempts to apply such biotechnologies in tile drainage systems were performed in Canada and the USA [7, 23, 89]. Subsequently, various later studies [7, 10, 15, 17] have suggested that application of these "nature-driven" measures can substantially reduce NO_3^- in drainage water.

Research-based knowledge is a prerequisite for a successful design of bioreactors. Therefore, the design of woodchip denitrification bioreactors has been studied at the laboratory on both pilot and field scales [2, 17, 31, 37, 58, 73].

Subsequently, various design approaches have been proposed. For instance, [16] suggested a bioreactor design method which is based on 10-20% peak drainage flow and hydraulic retention time of 6-7 hours. This approach has received much attention in practical applications in the Midwest of the United States. Another design concept correlated bioreactor surface area and treatment area allowing easier estimation of bioreactor volume [90].

The design approach based on nitrogen mass removal concept was proposed in [82]. There has been little discussion in the literature about the effect of bioreactor length-to-width ratio and cross-sectional shape on bioreactor performance. According to [16, 18], the highest bioreactor efficiency could be achieved when the ratio is around 10. The nitrate removal between trapezoidal and rectangular cross-sections does not show any significant differences. Overall, to date there is no consensus regarding the optimal drainage bioreactor design method and optimal bioreactor parameters [18]. Various methods result in different bioreactor sizes and efficiencies [18].

Although the number of investigations on denitrification process in woodchip bioreactors has significantly increased, a great interest to elaborate mathematical nitrate removal approach still remains relevant. Mathematical modelling can often be used for better assessment of chemical transport, optimization, estimation and design of pollutants removal operations [19]. Over the past decades, researchers have developed a number of mathematical models to simulate chemical transport of nitrates, oxygen and products of the reactions in the reactors. The majority of them were simplified to enzymatic conversion of nitrate in anaerobic media and kinetic rate (zero and first order) expressions.

The main purpose of this chapter is to present a mathematical model for the processes within the woodchip denitrification bioreactor applicable not only to simulate chemical transport of nitrates and oxygen, but also to control and optimize the nitrate conversion efficiency. The primary task of the model containing the control mechanism is to maintain the variable water flow for a required (set-point) output NO_3^- concentration. The model could serve as a tool for better bioreactor design.

The main goal of this approach was the creation of the mathematical model suitable to monitor the denitrification process in time. A pilot-scale cube-shape plastic denitrification bioreactor was used for the real experiments. The experiments were carried out under in turn flowing-through and non-flowing water conditions. Due to two types of experiments two mathematical models of denitrification process (for the non-flowing and for the flowing-through

conditions) were proposed and analyzed.

Models belong to a class of problems, namely differential equations subject to nonlocal conditions [85]. Nonlocal conditions describe the relationship between the solution values and the equation system parameters. The real experiments of the denitrification process were mathematically described as a systems of two convection–reaction equations, without regard to auxiliary conditions (turbulent flow, etc).

Systems of convection–reaction and convection–reaction–diffusion equations are usually used for the denitrification process modeling as well as for wastewater treatment and simulations of reactive settling of activated sludge [8]. A similar model with the added source of carbon was proposed in [55] to predict bacterial nitrate removal in groundwater. The suggested kinetic model combines Monod kinetics and a constant denitrification rate.

The experiment with non-flowing water conditions was analyzed first. Nitrate and dissolved oxygen concentrations were found through experiments. The constructed mathematical model allowed to calculate rate constants for the analyzed chemical reactions.

Afterwards, the system of differential equations was supplemented with a convection term. This improvement of the existing model with a non-flowing water condition along with the experimental data enabled to predict and calculate the treatment of flowing-through water, even without real experimentation.

Nonlocal conditions with convection represent the control mechanism. The process control has been analyzed in [41] using a PID (proportional–integral–derivative) controller [3]. A similar model was created using a PI (proportional–integral) controller. The controller in this model adjusts the water flow-through rate in order to satisfy the set-point outflow concentration. Application of PI control in the mathematical model enables the design of the intelligent treatment systems with variable inflow NO_3^- concentrations.

Materials, methods and processes

Field experiment

A pilot-scale cube-shaped plastic denitrification bioreactor (1.0 m^3 volume) was placed below the ground by the excavation of a 1.2 m trench constructed at

the Drainage Laboratory of Vytautas Magnus University, Lithuania (Fig. 3.1). The bioreactor's container was fed by water from two interconnected plastic water tanks (1.0 m^3 volume each). The container was filled with mixed woodchips made from local raw materials. Alder (*Alnus glutinosa*) and pine (*Pinus sylvestris*) tree scraps dominated in the woodchips with prevailing (at 65% of the cumulative distribution) particle diameter varying from 1.1 to 3.0 *cm* (bulk density of 260 kg/m^3). The bioreactor was filled with woodchips to a depth of 1.0 *m*, and a saturation level of 0.90 *m* was maintained. A polyethylene liner was also folded over the top of the bioreactor to seal it from the soil and a mound with a 20 *cm* thickness was formed and sown with grass. The woodchip porosity was determined using a standard porosity determination procedure described by [15]. The analysis revealed that woodchip porosity was 56%.

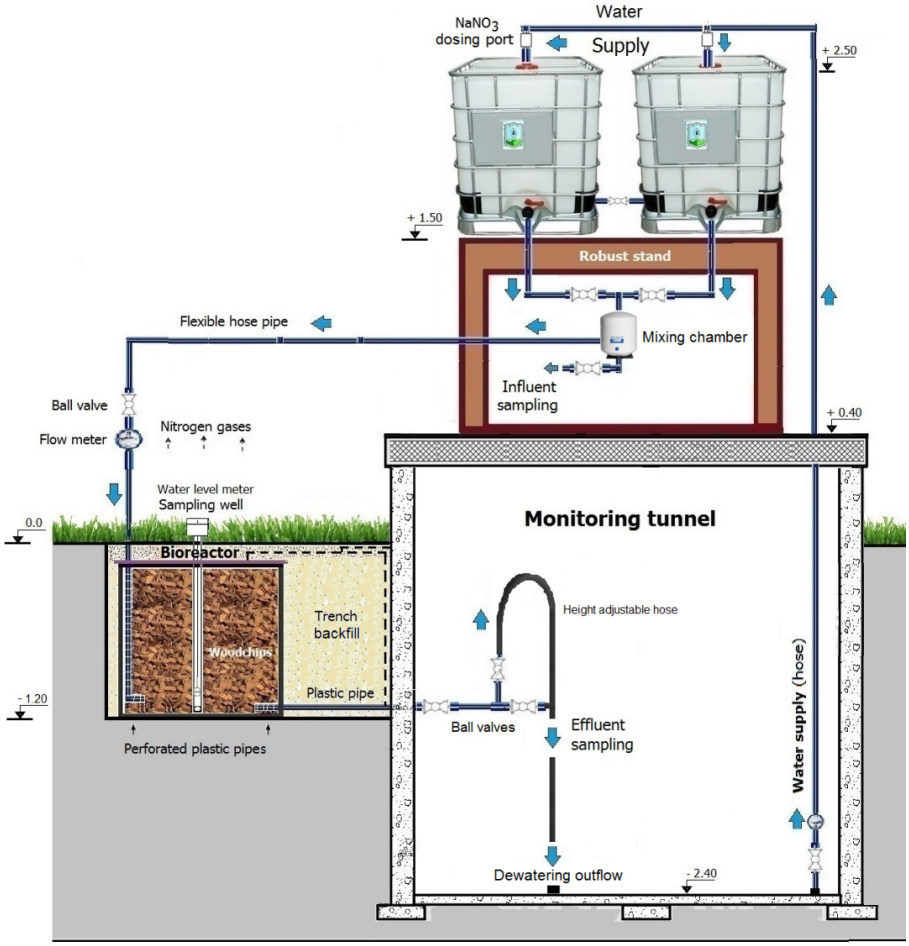

Figure 3.1: Schematic of the pilot-scale woodchip bioreactor [72]

The experiment was carried out under in turn flowing-through (average retention time = 3.10 hours calculated as the ratio between the bioreactor's pore volume and flow rate) and non-flowing water conditions. The NO_3^- removal efficiency (determined as the difference between the inlet and outlet NO_3^- concentrations divided by the inlet concentration) tests in the bioreactor started on July 20, 2017 and the results cover the period until June 10, 2018. The water from the tanks was supplied to the bioreactor by gravity. The flow rate was determined by the difference in hydraulic head (max 3.6 m) between the water levels in the tanks and in the bioreactor. The inflow and outflow rates were adjusted manually using valves. The bioreactor was fed with nitrate (via the addition of $NaNO_3$ to the water tanks) at concentrations ranging from 28.0 to 132.0 $mg \cdot L^{-1}$ with an average value of 66.1 $mg \cdot L^{-1}$. These concentrations are typical (83% of the cumulative frequency) of the range of NO_3^- values observed in drainage water under field conditions. The outflow concentrations ranged from 16.0 to 98.0 $mg \cdot L^{-1}$ (average of 42.4 $mg \cdot L^{-1}$). Therefore, the NO_3^- removal efficiency changed from 17.5% to 70.8% (average of 37.1%).

During the study period, the water temperature at the inlet and outlet ranged from 13.9°C to 19.4°C. The pH values in the inflow ranged from 5.2 to 8.6, and those of the outflow from 5.0 to 8.3. The dissolved oxygen concentrations at the inlet and outlet ranged from 3.2 to 4.4 $mg \cdot L^{-1}$ and from 0.0 to 1.2 $mg \cdot L^{-1}$ respectively.

The measurements were performed at various irregular time intervals varying from 16.43 to 183.3 hours by applying the same sampling procedures. In total, 41 experiments were carried out, the results of which were used in this chapter. Sampled at the outlet, nitrate and oxygen concentrations were measured at the beginning and at the end of the experiments. The presence of NO_3^- was determined via the spectrometric method using a Photometer MD600/MaxDirect (accuracy $\pm$ 0.5 $mg \cdot L^{-1}$) system with powder reagents. The dissolved oxygen content (accuracy $\pm$ 1.5%) and the water temperatures (accuracy $\pm$ 0.2 °C) were measured with a portable HI-9142 (Hanna® Instruments Ltd.) multimeter, and the pH values were registered by a HI-98136 meter (accuracy $\pm$ 0.1 pH).

Physical model

The model is constructed on the base of chemical processes in the bioreactor described in typical kinetics and competition equations [87].

Cellulose degrading microorganisms grow on woodchips and produce extracellular enzyme cellulase. This enzyme catalyzes the hydrolysis of cellulose, which produces soluble monosaccharides (usually glucose) and a variety of oligosaccharides of different lengths.

1. Cellulose + $H_2O \xrightarrow{Cellulase}$ glucose + oligosaccharides.
2. Glucose, oligosaccharides + $O_2 \xrightarrow{k_2} 6CO_2 + 6H_2O$.
3. Glucose, oligosaccharides + $NO_3^- \xrightarrow{k_1} N_2$ + Volatile N compounds + $nH^+ + mCO_2 + H_2O$.

Cellulase producing microorganisms grow in aerobic media. When oxygen is consumed, production of the enzyme stops. However, previously produced cellulase still works. Anaerobic cellulase producing microorganisms also exist. They consist of about 5-10% of aerobic cellulase producing microorganisms [59]. They produce extracellular huge protein complexes that adsorb on cellulose surface. They catalyse hydrolysis of cellulose, and, probably, further destruction of soluble sugars to acetic acid, or lactic acid. Complexes are strongly inhibited by glucose. Thus, the number and variety of soluble carbon sources depend on oxygen concentration.

Under anaerobic conditions some microorganisms can switch from oxygen to nitrate. A different number and variety of volatile nitrogen oxide products will be produced (the third path). This process will continue until the previously produced cellulase inactivates and no more soluble sugars will be produced. When nitrate has been consumed, some microorganisms can switch to sulphates. However, sulphates can only be consumed at very high concentration of sulphates. It means that the process of carbon consumption is complicated and the rate of carbon consumption cannot be expressed by one equation.

Due to the decrease of oxygen concentration, the production of soluble sugars will also decrease. Thus, for the optimal nitrate removal process a sufficient oxygen concentration is necessary.

The nitrate removal rate can be regulated by the change of flow rate through the bioreactor. At a very low flow rate all oxygen will be consumed at the inlet of the bioreactor, and the efficiency of the reactor will be low. By increasing the flow rate we will involve more of the bioreactor's content into the process, thus increasing the rate of nitrate consumption. At a high flow rate in the bioreactor the aerobic conditions will dominate and the rate of nitrate removal will be low. For the precise regulation of the nitrate removal, the concentration of the

nitrates and concentration of oxygen should be controlled at the outlet of the bioreactor. It will be used as an essential information for the effective regulation of the reactor using a PI controller.

Mathematical model

A mathematical model of the nitrate removal in the woodchip denitrification bioreactor that guarantees the required water purity was composed. The model is based on differential equations which were used for the analysis of the water treatment experimental results and the water treatment processes. The inverse problem for the system of convection–reaction equations was solved for the analysis of denitrification processes.

Since the process of water treatment involves complex chemical reactions, in this chapter the variation of nitrate and oxygen concentrations during water treatment was analyzed. Regression analysis was used to analyze the experimental results. The dependence of the parameters characterizing water treatment on temperature and pH was estimated. Water flow rates which allow to reduce the NO_3^- concentration to the desired level were presented.

The main chemical assumptions are: the oxygen concentration decreases exponentially and the NO_3^- concentration decreases nonlinearly during the water treatment process. Since the real experiments were conducted on non-flowing water conditions and woodchip porosity was 56%, an assumption was made that the medium can be considered to be homogeneous and it is sufficient to analyze the changes over time.

Non-flowing water model

First, the data from the non-flowing water experiments were analyzed. Every experiment was taken as a single observation in a given dataset. The variables and dimensions for each experiment are described in Table 3.1.

The non-flowing water experiments were used to analyze and compute the rate constants for the model, as well for the statistical analysis of the experiments. The inverse problem was solved for the system of two differential

equations supplementing the initial and boundary conditions:

$$\frac{dC_{NO_3}}{dt} = -k_1 C_{NO_3}\left(1 - \frac{C_{O_2}}{C_{NO_3}}\alpha\right), \tag{3.1a}$$

$$\frac{dC_{O_2}}{dt} = -k_2 C_{O_2}, \quad 0 < t \leq T, \tag{3.1b}$$

where k_1 - nitrate and k_2 – oxygen removal reaction rates (h^{-1}); α - oxygen domination *proportion*. Such system of nonlinear kinetic equations is often used to describe chemical reactions or interactions between substances [87].

The additional conditions for the inverse differential problem are formulated using concentrations at the beginning ($t = 0$) and at the end ($t = T$) of the experiment:

$$C_{NO_3}|_{t=0} = b_1, C_{O_2}|_{t=0} = d_1, \tag{3.2a}$$

$$C_{NO_3}|_{t=T} = b_2, C_{O_2}|_{t=T} = d_2. \tag{3.2b}$$

The system should be solved for the rate constants k_1, k_2. Nitrates are consumed relatively to the oxygen concentration decline:

$$\alpha = \frac{C_{NO_3}|_{t=0}}{C_{O_2}|_{t=0}}. \tag{3.3}$$

To start with the solution for each experiment, the value of k_2 was determined from the inverse problem (3.1b) with the initial conditions (3.2a) and the

Table 3.1: The parameters of experiments

T	experiment duration (h)
$C_{NO_3}\|_{t=0}$	NO_3^- concentration when experiment starts ($mg \cdot L^{-1}$)
$C_{NO_3}\|_{t=T}$	NO_3^- concentration when experiment ends ($mg \cdot L^{-1}$)
$C_{O_2}\|_{t=0}$	O_2 concentration when experiment starts ($mg \cdot L^{-1}$)
$C_{O_2}\|_{t=T}$	O_2 concentration when experiment ends ($mg \cdot L^{-1}$)
$temp$	average temperature (°C)
pH	water acidity (pH) when experiment ends

boundary conditions (3.2b):

$$k_2 = \frac{ln\frac{d_1}{d_2}}{T}. \tag{3.4}$$

k_1 was obtained from the optimization problem of differential equations (3.1a, 3.1b) with the initial conditions (3.2a) and the boundary conditions (3.2b). The initial guess of k_1^* was used for the optimization algorithm:

$$k_1^* = \frac{ln\frac{b_1}{b_2}}{T}. \tag{3.5}$$

Flowing-through water model

An additional parameter (water flow) was added to the model described in the previous chapter. The case when the water passes at a constant rate through the bioreactor is studied. The modeled bioreactor structure was assumed to be homogeneous with evenly distributed woodchips, laminar flow and unchanged inner distribution of microorganisms due to the flow.

The idea was to look for the water flow rates which would guarantee the required NO_3^- removal. The mathematical model based on the system of two convection–reaction equations (3.6) was applied.

The flow-through denitrification bioreactor mathematical model is defined as a system of two first order convection-reaction nonlinear differential equations:

$$\begin{aligned}
&\frac{\partial C_{NO_3}}{\partial t} = V\frac{\partial C_{NO_3}}{\partial x} - k_1 C_{NO_3}\left(1 - \frac{C_{O_2}}{C_{NO_3}}\alpha\right),\\
&\frac{\partial C_{O_2}}{\partial t} = V\frac{\partial C_{O_2}}{\partial x} - k_2 C_{O_2},\\
&(x,t) \in D = \{0 < x < a, 0 < t \leq T\},
\end{aligned} \tag{3.6}$$

where $C_{NO_3}(t,x)$ – NO_3^- concentration ($mg \cdot L^{-1}$); $C_{O_2}(t,x)$ – dissolved oxygen concentration ($mg \cdot L^{-1}$); k_1, k_2 – reaction rate constants (h^{-1}); α - oxygen domination proportion; t – time (h); V – water flow rate ($m \cdot h^{-1}$); a – length of denitrification bioreactor (m); T – reaction duration (h).

The initial conditions specify the concentration distribution inside the biore-

actor at the initial time moment ($t = 0$):

$$C_{NO_3}(t,x)|_{t=0} = c_1, \quad C_{O_2}(t,x)|_{t=0} = c_2, \quad 0 \le x \le a, \tag{3.7}$$

where c_1, c_2 – initial nitrate and dissolved oxygen concentrations ($mg \cdot L^{-1}$).

The boundary conditions define the nitrate and dissolved oxygen concentrations at the points of inlet during the reaction ($0 < t \le T$):

$$C_{NO_3}(t,a) = Cn = const, \quad C_{O_2}(t,a) = Co = const, \quad 0 < t \le T. \tag{3.8}$$

A set-point for the required NO_3^- concentration h at the point of outlet was determined:

$$C_{NO_3}(t,0) = h, \quad 0 < t \le T. \tag{3.9}$$

To find the solution of the system of differential equations with the initial and boundary conditions, the finite difference (explicit forward difference at time) methods [6, 76] and the Newton-Raphson (or secant) method for optimization [49] were used.

Flowing-through water model with monitoring

This mathematical model allows to compute the optimal water flow rate based on the nitrate inflow concentration.

The refined model allows for the variable inflow concentration control with a given set-point outflow concentration as an objective.

The mathematical model is very similar to the previous one. The differential equations are the same as (3.6), but the nonlocal condition representing the control mechanism is defined as a PI controller and the water flow rate V is a function of time t:

$$V(t) = \mathscr{K}_p e(t) + \mathscr{K}_i \int_0^t e(\tau) d\tau, \quad 0 < t \le T. \tag{3.10}$$

The controller adjusts the water flow-through rate $V(t)$ in this model to satisfy the set-point outflow concentration. $\mathscr{K}_p$, $\mathscr{K}_i$ are non-negative coefficients for a proportional and integral terms in a PI scheme. The error function $e(t)$ is

the difference between the required NO_3^- concentration and the measured one

$$e(t) = h - C_{NO_3}(t,0), \quad 0 < t \leq T. \tag{3.11}$$

The PI controller continuously evaluates the error value $e(t)$ and attempts to minimize it over time by adjusting the control variable $V(t)$ to a new value defined by (3.10). If $e(t) < 0$, the $V(t) = 0$ was accepted.

The principal scheme of the computational experiment is shown in Fig. 3.2.

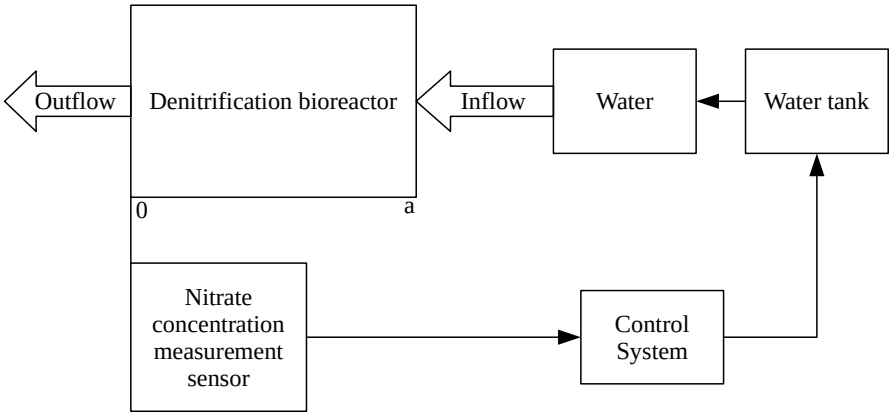

Figure 3.2: Principal scheme of the denitrification process under PI controller.

Results and discussion

The results obtained from the mathematical models and statistical analysis are presented in this section. The nitrate removal average rates are discussed as well. Experiments were performed under different water temperature, acidity (pH) and duration values.

Average nitrate removal rates

The nitrate and oxygen average removal rates are very important characteristics of the denitrification process. It is defined as

$$S_{NO_3} = \frac{C_{NO_3}|_{t=T} - C_{NO_3}|_{t=0}}{T},$$
$$S_{O_2} = \frac{C_{O_2}|_{t=T} - C_{O_2}|_{t=0}}{T}.$$

The experiment data was analyzed by statistical methods. The main statistical indicators are presented in Table 3.2. The minimal values of the experiment data are given in the first table column (T – experiment duration, $C_{NO_3}|_{t=0}$ – NO_3^- concentration at the beginning of the experiment, $C_{NO_3}|_{t=T}$ – NO_3^- concentration at the end of the experiment, etc.).

Table 3.2: Experiment data summary

	Min.	1st Qu.	Median	Mean	3rd Qu.	Max.
T	16.43	20.08	45.42	51.90	76.33	183.3
$C_{NO_3}\|_{t=0}$	28.00	50.00	55.00	63.66	70.00	132.0
$C_{NO_3}\|_{t=T}$	16.00	26.00	32.00	38.00	42.00	98.00
$C_{O_2}\|_{t=0}$	3.400	3.540	3.640	3.668	3.760	4.200
$C_{O_2}\|_{t=T}$	0.050	0.050	0.100	0.293	0.150	1.180
S_{NO_3}	0.212	0.335	0.645	0.730	1.054	1.877
S_{O_2}	0.020	0.048	0.084	0.098	0.139	0.217

The multiple linear regression for nitrate removal average rate S_{NO_3} and oxygen decline average rate S_{O_2} with respect to temperature and pH using the laboratory experiment data were computed. The linear model was used due to the narrow range of the parameters $temp$ and pH. The analysis is based on the data of 41 experiments.

A computed linear-fit model revealed weak dependence for S_{NO_3} and S_{O_2} on $temp$ and pH. Multiple R^2 for S_{NO_3} is 0.182, for S_{O_2} is 0.0722. This indicates there was no strong inter-dependency between the nitrate removal rate and fluctuations in temperature and pH. A previous investigation [73] shows that the nature of the woodchips does not have impact on the overall rate of nitrate removal. Therefore, it is proposed to use a control mechanism to ensure the

required nitrate concentration at the outflow.

Flow rate selection for the required nitrate outflow concentration

It is important to maximize the efficiency of the bioreactor. This can be achieved by monitoring the water flow rate. This section presents numerical results for the flow rate control. The computed flow rate ensures the required purity of the outflow water providing supreme flow rate.

In the experiments the nitrate inflow concentration $C_{NO_3}(t,a)$ was in the 28 – 132 $mg \cdot L^{-1}$ range. Having the upper and lower inflow concentration bounds, the corresponding flowthrough rate for the bioreactor with the outflow NO_3^- concentration was computed and set to 2.22 $mg \cdot L^{-1}$.

The choice of a set-point parameter was based on the fact of sulphate presence which can compete and act as an alternative electron acceptor when more reducing conditions develop. Consequently, a sulphate reduction normally occurs when NO_3^- - concentrations have been substantially depleted (below 2.22 mg/L) [82].

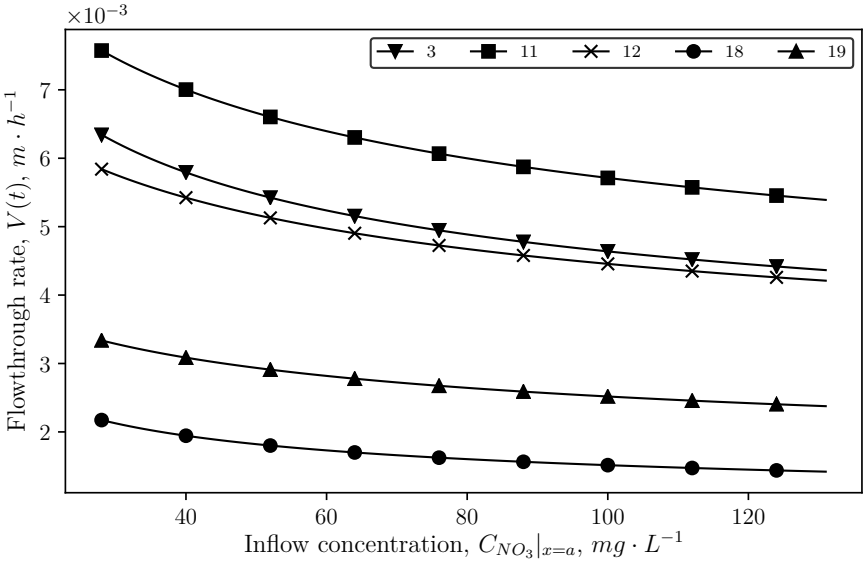

Figure 3.3: Computed inflow concentration dependency on the computed flowthrough rate. Each line corresponds to a single experiment. Each experiment is labeled with a number. The experimental data is presented in Table 3.3.

Table 3.3: Experiment data for Fig. 3.3

Experiment number	k_1, h^{-1}	k_2, h^{-1}	α
3	0.03606	0.2243	14.40
11	0.04492	0.2056	14.18
12	0.03520	0.1455	15.49
18	0.01160	0.1368	11.84
19	0.01980	0.0992	17.82

Fig. 3.3 shows the computed results of the mathematical model for five randomly picked experiments. For a given range of the NO_3^- concentration in the drainage water there can be found a flowthrough rate which allows to reach a safe outflow NO_3^- concentration (2.22 $mg \cdot L^{-1}$). Each experiment had its own set of parameters (Table 3.3).

From the results it follows that under a higher inflow NO_3^- concentration the flowthrough rate should be reduced. As an example the experiment number 12 was analyzed. Under a 40 $mg \cdot L^{-1}$ inflow concentration the flow rate cannot exceed $5.42 \times 10^{-3} m^3 \cdot h^{-1}$, but when the NO_3^- concentration exceeds 120 $mg \cdot L^{-1}$ the flowthrough rate should be limited to $4.29 \times 10^{-3} m^3 \cdot h^{-1}$.

Bioreactor length selection

For the purposes of water treatment, it is important to ensure that the water purity requirements are met while the outflow volume is maximized. In case the desired rate of outflow is fixed, this objective can be achieved by adjusting the length of the bioreactor.

The mathematical model can be used to calculate the length of the bioreactor which ensures the required outflow rate and 2.22 $mg \cdot L^{-1}$ nitrate concentration. For this purpose, the inverse problem for a system of differential equations (3.6) was solved at a given flow rate V.

The results of the numerical experiments showed linear dependence between the length of the bioreactor needed to maintain the "safe" NO_3^- concentration and the flowthrough rate.

The linear regression formula for a given dataset is (3.12) measured in m:

$$L = 72.5 \times V, \quad L \geq 1. \tag{3.12}$$

For example, if the reaction rates are $k_1 = 0.00970$ and $k_2 = 0.05809$, then the required flow rate of $1.38 \times 10^{-2} m/s$ is sufficient for the 1 m length bioreactor. Whereas for the 10 m length bioreactor, the maximum flow rate should not exceed $1.38 \times 10^{-1} m/s$. The width and length of the bioreactor are equal to 1 meter each.

Flow rate control for variable inflow concentration

The water treatment optimization is more difficult when the inflow water has a varying nitrate concentration. This section presents the results of calculations for a case where the input water nitrate concentration varies as a sinusoidal function. The results are presented in Fig. 3.4 and Fig. 3.5. In this particular case the inflow NO_3^- concentration varies between 55-82 $mg \cdot L^{-1}$. The outflow concentration is set to be maintained by the PI controller, the set-point is 2.22 $mg \cdot L^{-1}$.

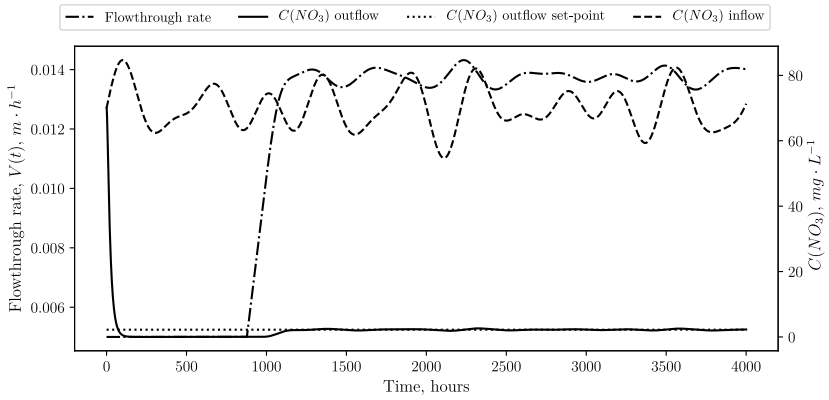

Figure 3.4: Computed flowthrough rate ($V(t)$, left axis). NO_3^- inflow and outflow concentrations (right axis). Obtained by using PI control for a periodically changing inflow concentration of NO_3^-.

The Fig. 3.5. shows the PI control result for a given parameter set. We can observe the outflow rate and NO_3^- concentration to be approximately the same function but shifted in time. It is due to a lag in the control signal and its propagation in NO_3^- concentration change. In this example the set-point and the actual measured concentration have a spread within 20%.

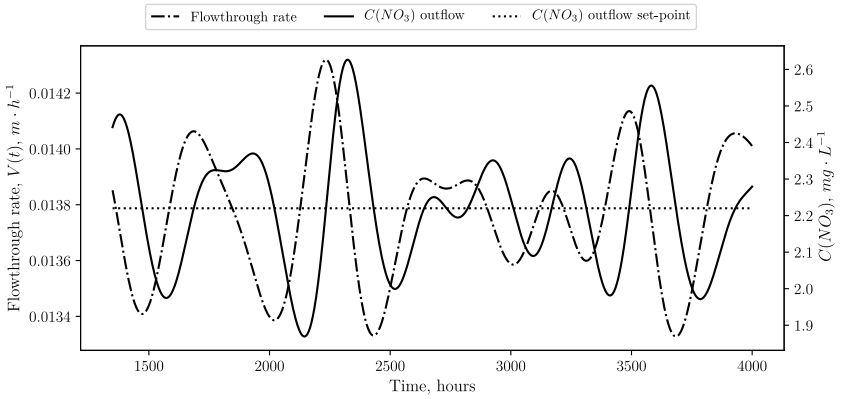

Figure 3.5: Time range from a Fig. 3.4 where the process control is within the "flat" range.

Conclusions

A series of field experiments for cube-shape plastic denitrification bioreactor were performed. The mathematical model of nitrate removal in a woodchip denitrification bioreactor based on the field experiments was proposed in this study. The variation of nitrate and oxygen concentrations during water treatment was analyzed in this chapter. The nitrate removal processes in a bioreactor were modeled under non-flowing and through-flowing conditions. The mathematical approach for denitrification process is a system of nonlinear differential equations describing the kinetic and convection processes.

The average nitrate removal rate S_{NO_3} and the oxygen decline average rate S_{O_2} were calculated for each field experiment. The chemical reaction rates (k_1 and k_2) of denitrification process were calculated by solving the inverse problem for the differential system for each field experiment.

The linear regression formulae for the nitrate removal average rate S_{NO_3} and the oxygen decline average rate S_{O_2} as well as for the chemical reaction rates (k_1 and k_2) of denitrification process with respect to temperature and pH were obtained.

Two methods have been proposed to maximize the efficiency of a bioreactor by monitoring the water flow rate.

A mathematical formula for bioreactor length selection is presented when the NO_3^- concentration of the inflow and the flow rate are known. The computed

length ensures the required purity of the outflow water.

A sophisticated mathematical algorithm for flow rate selection is presented. The NO_3^- concentration at inlet varies over time. The distinctive feature of this model is the nonlocal condition representing the control mechanism which is defined as a PI controller. The water flow rate is a function of time.

4. Study of difference scheme for a system of nonlinear reaction-diffusion equations with control

This chapter is based on the manuscript which is the result of original research submitted to the journal *Applied Mathematics and Computation*.

Introduction and problem statement

Many physical phenomena have been formulated as mathematical models with nonlocal boundary conditions of various types. In the last few decades, the development of numerical methods for the solutions of nonlocal boundary value problems has been an important research area in many branches of applied science. A short overview of these models is presented in many papers (see for example [21, 25, 62, 85] and references therein).

For example, one of such mathematical models with nonlocal conditions is the reaction-diffusion equation in connection with its applications in chemical diffusion, electrochemistry, dynamics of various bioreactors, mathematical biology, some inverse problems and other applications [20, 41, 63, 65, 67, 83].

One of the first mathematical models with a nonlocal condition has been published in [11]. In this chapter, a nonlocal condition instead of one boundary value condition $u(0,t) = \mu(t)$ has been formulated for the heat condition equation

$$\frac{\partial U}{\partial t} = \frac{\partial^2 U}{\partial x^2}, \quad 0 < x < 1, \quad 0 < t \leq T\,. \tag{4.1}$$

$$\int_0^{x(t)} u(x,t) = E(t), \tag{4.2}$$

where $x(t)$ and $E(t)$ are given functions. There is an obvious interpretation of this nonlocal condition. For example, if $u(x,t)$ denotes temperature in a heat conduction problem, then $E(t)$ represents an internal energy content of the

region $0 < x < x(t)$ at time t. Likewise, if $u(x,t)$ denotes the concentration of a chemical substance for a diffusion process, then $E(t)$ represents the mass of this substance that is present in the region $0 < x < x(t)$ at time t.

The nonlocal conditions arise usually when it is impossible to determine the boundary values of the solution at some boundary points. These conditions are typical for some inverse and control problems.

In the present chapter, a one-dimensional mathematical model [51] to simulate the dynamics of a bioreactor is considered. The system of two parabolic nonlinear reaction-diffusion equations with a diffusion and enzymatic reaction is presented:

$$\frac{\partial S}{\partial t} = \mathscr{D}_S \frac{\partial^2 S}{\partial x^2} - \frac{V_{max} S}{K_M + S + S^2/\overline{Y_u}}, \quad 0 < x < d \tag{4.3}$$

$$\frac{\partial P}{\partial t} = \mathscr{D}_P \frac{\partial^2 P}{\partial x^2} + \frac{V_{max} S}{K_M + S + S^2/\overline{Y_u}}, \quad 0 < t \leq T, \tag{4.4}$$

where x stands for space, t stands for time, $S(x,t)$, $P(x,t)$ are the concentration of the substrate and reaction product respectively, d is the thickness of bioreactor, V_{max} is the maximal enzymatic rate. K_M and $\overline{Y_u}$ are the Mechaelis-Menten and the inhibition constants respectively, $\mathscr{D}_S$ and $\mathscr{D}_P$ are the diffusion coefficients of the substrate and the reaction product respectively.

The initial condition represents an empty bioreactor, where neither a product nor a substrate is present. It means that

$$P(x,0) = 0, \quad S(x,0) = 0, \quad x \in [0,d]. \tag{4.5}$$

In order to define a full mathematical model, three boundary conditions can be rewritten

$$P(0,t) = 0, \quad \frac{\partial P(d,t)}{\partial x} = 0, \quad \frac{\partial S(0,t)}{\partial x} = 0, \quad 0 < t \leq T. \tag{4.6}$$

The first condition means that product outflow is allowed. The next two conditions mean that the product P at $x = d$ and the substrate S at $x = 0$ cannot flow respectively. The last condition specifies the flux of P at the boundary $x = 0$:

$$\mathscr{D}_P \frac{\partial P(0,t)}{\partial x} = Q(t), \quad 0 < t \leq T, \tag{4.7}$$

where $Q(t)$ defines the flux of the drug prescribed by a doctor in accordance

with the therapeutic protocol (the objective function of the optimization task).

It is clear that such combination of boundary conditions (4.6), (4.7) is not typical for the classical well-posed boundary value problem. In order to use such bioreactors in real life applications, it was proposed [41] to find the equivalent boundary condition for the substrate function $S(d,t) = S_0(t)$.

For this purpose, the error function is defined

$$e(t) = Q(t) - \mathscr{D}_P \frac{\partial P(0,t)}{\partial x}, \quad 0 < t \leq T, \tag{4.8}$$

which defines the difference between the required product outflow $Q(t)$ and the real product outflow. In order to minimize the value of $|e(t)|$ the "I" control is used [28],

$$S(d,t) = K_c \int_o^t e(\tau) d\tau, \quad 0 < t \leq T. \tag{4.9}$$

To solve the problem (4.3)-(4.7) the condition (4.7) with the nonlocal boundary condition is changed

$$S(d,t) = K_c \int_o^t \big(Q(t) - \mathscr{D}_P \frac{\partial P(0,t)}{\partial x}\big) dt, \quad 0 < t \leq T. \tag{4.10}$$

The system of diffusion-reaction equations (4.3), (4.4) belongs to the class of partial differential equations which are used widely for investigation of different types of bioreactors and biosensors. The system of diffusion-reaction equations (4.3), (4.4) describes the action of the non-steady state biosensor at mixed enzyme kinetics, external and internal diffusion limitation with substrate inhibition [35, 50]

The system of nonlinear differential equations (4.3), (4.4) with initial conditions (4.5) and boundary conditions (4.6), (4.10) is considered.

From the mathematical point of view, the author's objective in this chapter is to solve the system of nonlinear differential equations (4.3), (4.4) subject to nonlocal conditions (4.10) by applying the finite difference method. Moreover, the main goal is to consider the stability of the difference scheme. To this end, the structure of spectrum of the difference operator is considered. Such method of investigation of the stability of the difference problem in the case of nonlocal conditions has been used in many papers [9, 33, 34, 38, 77, 79].

Please note that the structure of spectrum of difference operators can be rather complicated even in the case of a simple nonlocal condition. Furthermore, this structure strongly depends not only on the type of the nonlocal condition

but also on the values of function parameters in the nonlocal conditions [34, 69, 78–81, 85]. The structure of the spectrum of difference operators with nonlocal conditions is closely related to the stability of the difference schemes for parabolic equations.

In the nonlocal condition (4.10) the value $S(d,t)$ of the solution $S(x,t)$ is expressed by the derivative of the solution $P(x,t)$ with respect to x in the whole range $[0,t]$. As far as the author knows, nonlocal conditions of this form have not been previously studied. The spectrum of a difference operator with such a nonlocal condition of this form has not been studied so far. Therefore, the theoretical stability study with the results of a numerical experiment is supplemented.

It was also noticed that problems with nonlocal conditions quite often fail to investigate the stability of difference schemes in the usual norms C or L_2. Therefore, special energy norms are used [33, 77].

In this chapter, the existence of the solution of the difference problem is studied as well as the issues of uniqueness and stability assuming that the solution of the differential problem exists, is unique and quite smooth.

Difference scheme

The differential problem (4.3)-(4.6),(4.10) is approximated by the forward Euler finite difference scheme. It is started by dividing the intervals $x \in [0,d]$ and $t \in [0,T]$ into an $N \times M$ mesh with step sizes $h = d \,/\, N$ and $\tau = T \,/\, M$. Let's denote $S_i^n = S(ih, n\tau)$ and $P_i^n = P(ih, n\tau)$ as the solutions of the difference problem.

From now, the differential problem with the following difference scheme is approximated:

$$\frac{S_i^{n+1} - S_i^n}{\tau} = \mathscr{D}_S \frac{S_{i-1}^n - 2S_i^n + S_{i+1}^n}{h^2} - \frac{V_{max} S_i^n}{K_M + S_i^n + (S_i^n)^2 / Y_u}, \tag{4.11}$$

$$i = 1, ..., N-1; \quad n = 0, 1, ..., M-1; \tag{4.12}$$

$$\frac{P_i^{n+1} - P_i^n}{\tau} = \mathscr{D}_P \frac{P_{i-1}^n - 2P_i^n + P_{i+1}^n}{h^2} - \frac{V_{max} S_i^n}{K_M + S_i^n + (S_i^n)^2 / Y_u}, \tag{4.13}$$

$$i = 1, ..., N-1; \quad n = 0, 1, ..., M-1; \tag{4.14}$$

$$P_0^{n+1} = 0, \quad n = 0,1,...,M-1. \tag{4.15a}$$

$$\frac{P_N^{n+1} - P_{N-1}^{n+1}}{\tau} = 0, \quad or \quad P_N^{n+1} = P_{N-1}^{n+1}, \quad n = 0,1,...,M-1, \tag{4.15b}$$

$$\frac{S_1^{n+1} - S_0^{n+1}}{\tau} = 0, \quad or \quad S_0^{n+1} = S_1^{n+1}, \quad n = 0,1,...,M-1. \tag{4.15c}$$

$$P_i^0 = 0, \quad i = 0,1,...,N; \tag{4.16a}$$

$$S_i^0 = 0, \quad i = 0,1,...,N-1; \tag{4.16b}$$

$$S_N^0 = \widetilde{S}, \tag{4.16c}$$

where $\widetilde{S}$ is the initial substrate concentration,

$$S_N^{n+1} = K_c \tau \sum_{j=0}^{n} \left(Q^j - \mathscr{D}_P \frac{P_1^j - P_0^j}{h} \right), \quad n = 0,1,\cdots,M-1. \tag{4.17}$$

The formulas (4.12), (4.14) correspond to the classical forward Euler scheme. The formula (4.17) can be interpreted as a left-hand rectangle rule of numerical integration in the interval $t \in [0, t^{n+1}]$. This form of approximate integration was chosen to keep the explicit forward Euler scheme for the case of the nonlocal condition (4.10).

At each time step $t = t^{n+1}$, the solutions S_i^{n+1} and P_i^{n+1} at all mesh points $i = 0,1,...,N$ are given by explicit formulas. That means, given S_i^n and P_i^n the equations (4.12)-(4.14) can be used to compute S_i^{n+1} and P_i^{n+1}, $i = 1,2,...,N-1$. Then, from the formulas (4.15a)-(4.15c) the values P_0^{n+1}, P_N^{n+1} and S_0^{n+1} are received. The final step is to calculate S_N^{n+1} from the nonlocal condition (4.17).

An important conclusion follows from this numerical algorithm.

Corollary 4.2.1. *The differential scheme (4.12)-(4.17) always defines a unique solution* $S_i^n, P_i^n, i = 0,1,\cdots,N, n = 0,1,\cdots,M$.

Stability of the difference scheme

The stability of a differential scheme is one of the most important aspects of the numerical method from both practical and theoretical points of view. Stability is a necessary condition for the convergence of the difference scheme.

The stability of difference schemes for one-dimensional linear parabolic equation with nonlocal conditions has been studied for a long time. Various research methods are described in articles [9, 12, 26, 38]. As already mentioned in Section 4.1, special energy vector norms are used to study the stability of difference schemes with nonlocal conditions. Let's write the standard two-layer difference scheme in the form:

$$u^{n+1} = \mathscr{G} u^n + f^n, \tag{4.18}$$

where u^n is an N-dimensional vector, $\mathscr{G}$ is a matrix of order N, usually nonsymmetric. Let's introduce the matrix

$$M = \langle \mu_1 \mu_2 \cdots \mu_N \rangle,$$

where columns are the eigenvectors and the associated vectors of the matrix $\mathscr{G}$. A symmetric positive definite matrix $\mathscr{D}$ is defined:

$$\mathscr{D} = (MM^*)^{-1},$$

where M^* as usual is the conjugate matrix.

The stability of a difference scheme with nonlocal conditions can be proven in a vector norm

$$\|u\|_{\mathscr{D}} = (\mathscr{D}u, u)^{\frac{1}{2}}, \tag{4.19}$$

which is called the energy norm generated by the positive definite matrix $\mathscr{D}$ [33].

The meaning of the norm $\|u\|_{\mathscr{D}}$ will be explained. Suppose, for simplicity, that $\mathscr{G}$ is a matrix of simple structure i.e. it has N linearly independent eigenvectors. Now, the norm of any matrix A can be defined in this way [22]

$$\|A\|_* = \|M^{-1} A M\|_2,$$

where $\|A\|_2 = \left(\max\limits_{1\le i\le N} \lambda_i(AA^*)\right)^{1/2}$ is the classical matrix norm.

This definition of the norm gives a simple expression of the norms of the matrix $\mathscr{G}$

$$\|\mathscr{G}\|_* = \|M^{-1}\mathscr{G}M\| = \|J\|_2 = \rho(\mathscr{G}), \tag{4.20}$$

where $J = diag(\lambda_1, \lambda_2, \ldots, \lambda_N)$, λ_i are the eigenvalues of the matrix $\mathscr{G}$, $\rho(\mathscr{G})$ is the spectral radius of $\mathscr{G}$, i.e.

$$\rho(\mathscr{G}) = \max_{1\le i\le N} |\lambda_i(\mathscr{G})|.$$

The compatible vector norm is defined by the formula [22]:

$$\|u\|_* = (M^{-1}u, M^{-1}u)^{\frac{1}{2}}. \tag{4.21}$$

Please note that in case when $\mathscr{G}$ is a matrix of simple structure the norm (4.19) coincides with the definition of the norm (4.21). Indeed,

$$\|u\|_* = (M^{-1}u, M^{-1}u)^{\frac{1}{2}} = \left((M^{-1})^* M^{-1}u, u\right) = \left((MM^*)^{-1}u, u\right)^{\frac{1}{2}} = \|u\|_{\mathscr{D}}.$$

Thus, the matrix norm (4.20) can be used to study the stability of the difference scheme (4.18), regardless of whether the matrix $\mathscr{G}$ is symmetric or not. From this it follows that the study of the spectrum structure of the difference operator with nonlocal conditions has become one of the major methods for the study of stability of difference schemes. For various one-dimensional linear parabolic equations the stability conditions of the difference schemes were investigated by this method. These results can be summarized in the following conclusion.

Corollary 4.3.1. *The backward Euler difference scheme with nonlocal conditions*

$$\frac{u^{n+1} - u^n}{\tau} = Au^{n+1} + f^n$$

is unconditionally stable if $Re\lambda(A) > 0$ *(it means that* $\rho\left((I - \tau A)^{-1}\right) < 1$*). For details, see for example [34, 57, 79, 80].*

The important property of the matrix norm (4.20) is that in case $\rho(S) > 1$ the difference scheme is not stable in any vector norm [9, 34].

Remark 4.3.2. Please note that it is possible to define the matrix norm with the property $\|\mathscr{G}\| = \rho(\mathscr{G})$ under the condition that $\mathscr{G}$ is a matrix of simple structure. In general, it is possible to define the matrix norm with the property $\|\mathscr{G}\| < 1$ if and only if $\rho(\mathscr{G}) < 1$ [5]. In this case, the compatible norm of the vector is defined in a more complicated way (see e.g., [5], Ch. 7.3 or [75] Ch II.2, par. 3.4). In any case, the sufficient condition of the stability of the difference scheme (4.18) in the norm $\|u\|_*$ is $\rho(\mathscr{G}) < 1$. $\square$

Recall that Corollary 4.3.1 is correct when the parabolic equation is linear. There are only a few articles in which the stability of difference schemes is theoretically investigated for nonlinear parabolic equations with nonlocal conditions [21, 29, 60, 67]. In [21], the stability is studied based on the spectrum structure of the differential operator.

The stability of the difference scheme (4.12)-(4.17) is analyzed based on the spectrum structure of the difference operator under the assumption $S << K_M, S^2 << Y_u$ (Corollary 4.3.1).

In this case, the differential equations (4.3), (4.4) are transformed into

$$\frac{\partial S}{\partial t} = \mathscr{D}_S \frac{\partial^2 S}{\partial x^2} - \frac{V_{max}}{K_M} S, \tag{4.22}$$

$$\frac{\partial P}{\partial t} = \mathscr{D}_P \frac{\partial^2 P}{\partial x^2} + \frac{V_{max}}{K_M} S. \tag{4.23}$$

Instead of the difference equations (4.12), (4.14) we obtain

$$\frac{S_i^{n+1} - S_i^n}{\tau} = \mathscr{D}_S \frac{S_{i-1}^n - 2S_i^n + S_{i+1}^n}{h^2} - \frac{V_{max}}{K_M} S_i^n, \tag{4.24}$$

$$i = 1, ..., N-1; \quad n = 1, ..., M-1; \tag{4.25}$$

$$\frac{P_i^{n+1} - P_i^n}{\tau} = \mathscr{D}_P \frac{P_{i-1}^n - 2P_i^n + P_{i+1}^n}{h^2} + \frac{V_{max}}{K_M} S_i^n, \tag{4.26}$$

$$i = 1, ..., N-1; \quad n = 1, ..., M-1; \tag{4.27}$$

A two level difference scheme (4.25), (4.27), (4.15a)-(4.17) will be defined in matrix form. To that end, let's first list all the equations of this system of difference equations in the following order

$$S_i^{n+1} = S_i^n + \tau\Big(\mathscr{D}_S \frac{S_{i-1}^n - 2S_i^n + S_{i+1}^n}{h^2} - \frac{V_{max}}{K_M} S_i^n\Big), \tag{4.28}$$

$$i = 1, ..., N-1; \quad n = 1, ..., M-1; \tag{4.29}$$

where $S_0^n = S_1^n$;

$$S_N^{n+1} = K_c \tau \sum_{j=0}^{n} \Big(Q^j - \mathscr{D}_P \frac{P_1^j - P_0^j}{h}\Big), \quad n = 0, 1, \cdots, M-1, \tag{4.30}$$

where $P_0^n = 0$;

$$P_i^{n+1} = P_i^n + \tau\Big(\mathscr{D}_P \frac{P_{i-1}^n - 2P_i^n + P_{i+1}^n}{h^2} + \frac{V_{max}}{K_M} S_i^n\Big), \tag{4.31}$$

$$i = 1, ..., N-1; \quad n = 1, ..., M-1; \tag{4.32}$$

where $P_0^n = 0$, $P_N^n = P_{N-1}^n$.

The equation (4.30) is rewritten into the equivalent form which follows from (4.30) by subtraction $S_N^{n+1} - S_N^n$.

$$S_N^{n+1} = S_N^n + \tau\Big(- \mathscr{D}_P K_c \frac{P_1^n - P_0^n}{h}\Big) + \tau K_c Q^n.$$

Let's define the following vectors and matrices: an N-dimensional vector S^n and an $(N-1)$-dimensional vector P^n

$$S^n = \{S_1^n, S_2^n, \cdots, S_{N-1}^n, S_N^n\},$$
$$P^n = \{P_1^n, P_2^n, \cdots, P_{N-1}^n\},$$

a square tridiagonal matrix Λ_1 of the order N

$$\Lambda_1 = \begin{pmatrix} a_1+b_1 & -a_1 & & & & \\ -a_1 & 2a_1+b_1 & -a_1 & & & \\ & -a_1 & 2a_1+b_1 & -a_1 & & \\ & & \ddots & \ddots & \ddots & \\ & & & -a_1 & 2a_1+b_1 & -a_1 \\ 0 & 0 & \cdots & 0 & 0 & 0 \end{pmatrix},$$

where $a_1 = \dfrac{\mathscr{D}_S}{h^2}$, $b_1 = \dfrac{V_{max}}{K_M}$; a square tridiagonal matrix Λ_2 of the order $N-1$

$$\Lambda_2 = \begin{pmatrix} 2a_2 & -a_2 & & & \\ -a_2 & 2a_2 & -a_2 & & \\ & -a_2 & 2a_2 & -a_2 & \\ & & \ddots & \ddots & \ddots \\ & & & -a_2 & 2a_2 & -a_2 \end{pmatrix},$$

where $a_2 = \dfrac{\mathscr{D}_P}{h^2}$; a rectangular matrix $\mathscr{D}_1$ of the order $N \times (N-1)$

$$\mathscr{D}_1 = \begin{pmatrix} 0 & 0 & 0 & \cdots & 0 & 0 & 0 \\ 0 & 0 & 0 & \cdots & 0 & 0 & 0 \\ \vdots & \vdots & \ddots & \ddots & \ddots & \vdots & \vdots \\ 0 & 0 & 0 & \cdots & 0 & 0 & 0 \\ b_2 & 0 & 0 & \cdots & 0 & 0 & 0 \end{pmatrix},$$

where $b_2 = \dfrac{V_{max}}{K_M}$ and a rectangular matrix $\mathscr{D}_2$ of the order $(N-1) \times N$

$$\mathscr{D}_2 = \begin{pmatrix} -b_1 & 0 & 0 & \cdots & 0 & 0 & 0 \\ 0 & -b_1 & 0 & \cdots & 0 & 0 & 0 \\ 0 & 0 & -b_1 & \cdots & 0 & 0 & 0 \\ \vdots & \vdots & \ddots & \ddots & \ddots & \vdots & \vdots \\ 0 & 0 & 0 & \cdots & -b_1 & 0 & 0 \\ 0 & 0 & 0 & \cdots & 0 & -b_1 & 0 \end{pmatrix}.$$

The system of difference equations (4.29)-(4.32) can now be written in the

form (4.33)

$$\begin{pmatrix} S^{n+1} \\ P^{n+1} \end{pmatrix} = \begin{pmatrix} S^n \\ P^n \end{pmatrix} - \tau \begin{pmatrix} \Lambda_1 & \mathscr{D}_1 \\ \mathscr{D}_2 & \Lambda_2 \end{pmatrix} \begin{pmatrix} S^n \\ P^n \end{pmatrix} + \tau \begin{pmatrix} F_1 \\ F_2 \end{pmatrix}, \tag{4.33}$$

where the N-dimensional vector F_1 and the $(N-1)$-dimensional vector F_2 are

$$F_1 = (0,0,\cdots,0,b_1)^T, \quad F_2 = (0,0,\cdots,0)^T.$$

Finally, the difference scheme (4.25), (4.27) with conditions (4.15a)-(4.17) is written in the following form

$$u^{n+1} = (I - \tau A)u^n + \tau f, \tag{4.34}$$

where I is an identity matrix,

$$u^n = \begin{pmatrix} S^n \\ P^n \end{pmatrix}, \quad A = \begin{pmatrix} \Lambda_1 & \mathscr{D}_1 \\ \mathscr{D}_2 & \Lambda_2 \end{pmatrix}, \quad f = \begin{pmatrix} F_1 \\ F_2 \end{pmatrix}.$$

The stability of this difference scheme will be investigated by proving a statement analogous to Corollary 4.3.1.

Theorem 4.3.3. *If $Re\lambda(A) > 0$ and $|Im\lambda(A)| \le |Re\lambda(A)| \le C/h^2$, then the difference scheme (4.34) is conditionally stable in the norm $\|u\|_*$, under the condition $\tau \le \frac{h^2}{C}$.*

Proof. According to Remark 1, the stability condition $\rho(I - \tau A) < 1$ of the difference scheme (4.34) will be used. When this condition is satisfied, it will be investigated. Let's denote $\lambda(A) = Re\lambda(A) + i \cdot Im\lambda(A)$. The evaluation of $|\lambda(I - \tau A)|$:

$$|\lambda(I - \tau A)| = |1 - \tau\lambda(A)| = |1 - \tau Re\lambda(A) - i\tau Im\lambda(A)| =$$

$$\Big(\big(1 - \tau Re\lambda(A)\big)^2 + \big(\tau Im\lambda(A)\big)^2\Big)^{1/2} =$$

$$\Big(1 - 2\tau Re\lambda(A) + \tau^2\Big(\big(Re\lambda(A)\big)^2 + \big(Im\lambda(A)\big)^2\Big)\Big)^{1/2}.$$

This expression will be less than one if

$$-1 < -2\tau Re\lambda(A) + \tau^2\Big(\big(Re\lambda(A)\big)^2 + \big(Im\lambda(A)\big)^2\Big) < 0.$$

The left-hand inequality is satisfied for all $\tau > 0$. It follows from the right-hand inequality that

$$\tau < \frac{2Re\lambda(A)}{\big(Re\lambda(A)\big)^2 + \big(Im\lambda(A)\big)^2}. \tag{4.35}$$

According to the assumptions of the Theorem $|Im\lambda(A)| \leq |Re\lambda(A)|$, hence the condition (4.35) will be true if

$$\tau \leq \frac{2Re\lambda(A)}{2\big(Re\lambda(A)\big)^2} = \frac{1}{Re\lambda(A)}.$$

Again, according to the assumptions of the theorem, the last inequality will be satisfied if

$$\frac{\tau}{h^2} \leq \frac{1}{C}.$$

Now, from inequality $|\lambda(I-\tau A)| < 1$ it follows that $\rho(I-\tau A) < 1$. □

Remark 4.3.4. The condition $|Im\lambda(A)| \leq |Re\lambda(A)|$ is only sufficient but not necessary for the stability of the difference scheme (4.34). In fact, it is only needed to ensure the conditional stability through the inequality $\tau/h^2 \leq 1/C$. But $Re\lambda > 0$ is the necessary condition of stability. When $Re\lambda(A) \leq 0$ and $Im\lambda(A) \neq 0$, then $\rho(I-\tau A) > 1$ for all values of τ. When $Re\lambda(A) > 0$, then the differential scheme (4.34) is conditionally stable for any value of $Im\lambda(A)$, under the condition (4.35) □

Remark 4.3.5. The assumptions $|Im\lambda(A)| \leq C/h^2$ and $Re\lambda(A) \leq C/h^2$ follow from the inequality $|\lambda(A)| \leq \|A\|_\infty = \max\limits_{1\leq i\leq n} \sum\limits_{j=1}^{n} |a_{ij}|$. In each particular case, only the constant C can change. □

Numerical results

To demonstrate and supplement the theoretical results, numerical experiments were performed. The numerical experiment was carried out to demonstrate the dependence of $minRe\lambda(\lambda)$ on K_c and V_{max}. The "I" control numerical solution analysis for the control parameter K_c was performed.

A numerical modeling was performed using a computer program developed by the author. It implements an explicit finite difference scheme using a forward difference in time and a second-order central difference for the space derivative.

The system parameters are: $\mathscr{D}_S = 5 \times 10^{-6}\, m^2 \cdot s^{-1}$, $\mathscr{D}_P = 5 \times 10^{-6}\, m^2 \cdot s^{-1}$, $V_{max} = 1.1 \times 10^{-3}\ mol \cdot m^{-3}$, $K_M = 0.2\ mol \cdot m^{-3}$, $d = 5 \times 10^{-3}\, m$.

Eigenvalue analysis

The numerical experiments related to the study of the stability of the difference scheme was performed. For this purpose, for a fixed value of h, all the eigenvalues of the matrix A were calculated. In other words, by changing the coefficients K_c, V_{max} values, it was observed that the property $Re\lambda(A) > 0$ was retained.

Fig. 4.1 and Fig. 4.2 provide the charts showing the dependence of $minRe\lambda(A)$ on K_c and V_{max}.

In the first chart (Fig. 4.1), the dependence of the control parameter K_c and the minimal value of the real parts of complex eigenvalues is presented. The most important region of this chart is the zero crossing area. At this point and to the right the stability of numerical algorithm for a given model with corresponding parameters cannot be guaranteed.

The second chart (Fig. 4.2) presents the results of the numerical experiment for the dependency of a V_{max} (the maximal enzymatic rate) and the minimal value of the real parts of complex eigenvalues. The same conclusion as the one in the result from Fig. 4.1 can be made, namely that in the zero crossing region and the part where the line is entering negative values the stability of numerical algorithm cannot be guaranteed.

From these numerical results it can be concluded that the difference scheme is stable $(Re\lambda(A) > 0)$ in a sufficiently wide range of coefficients K_c and V_{max}.

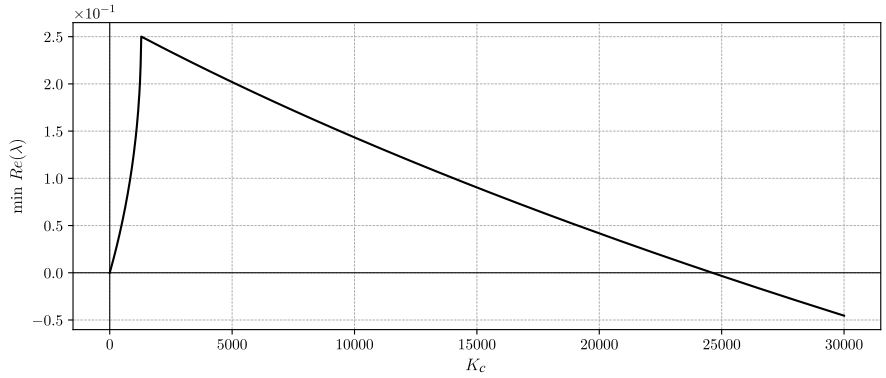

Figure 4.1: The dependency of a K_c and the $minRe(\lambda)$. Stability region of the difference scheme is within the range of positive values of $minRe(\lambda)$.

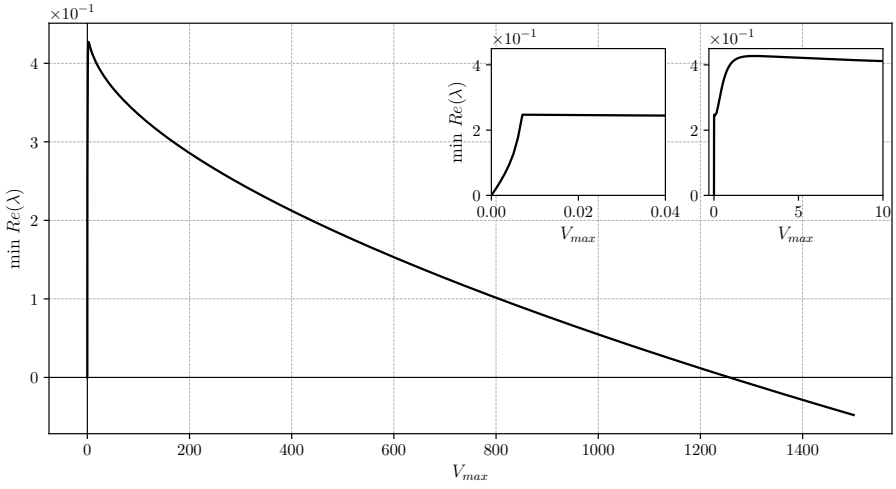

Figure 4.2: The dependency of a V_{max} and the $minRe(\lambda)$. Stability region of difference scheme is within the range of positive values of $minRe(\lambda)$.

Result of I control

In this part, the I (PID control partial case) control numerical solutions analysis for the control parameter K_c was performed. It was found that an interval of control parameter values (0, K_{c1}), where the model behavior is correct, K_{c1} depends on model parameters (V_{max}, K_M, Q, etc.). The model with control parameter K_c outside the interval (0, K_{c1}) can yield unpredictable results. For example, the concentration of a substrate or product at some point in time

can go negative which cannot be seen in the real world.

In all present stability studies, it was observed that the interval of control parameter K_c guaranteeing the numerical method stability ($Re\lambda(A) > 0$) is wider than the interval $(0, K_{c1})$.

Here two examples are presented where the control parameter K_c is within the interval $(0, K_{c1})$ and outside of it. The nonlinear system solution with control parameter K_c from the interval $(0, K_{c1})$ is presented in Fig. 4.3. Here the substrate concentration is rising slowly with a slight overshot starting from the 18th second, which in this case is negligibly small and acceptable. Settlement is observable from the 35th second and the following constant rate matching of the set-point is the goal of this particular control system.

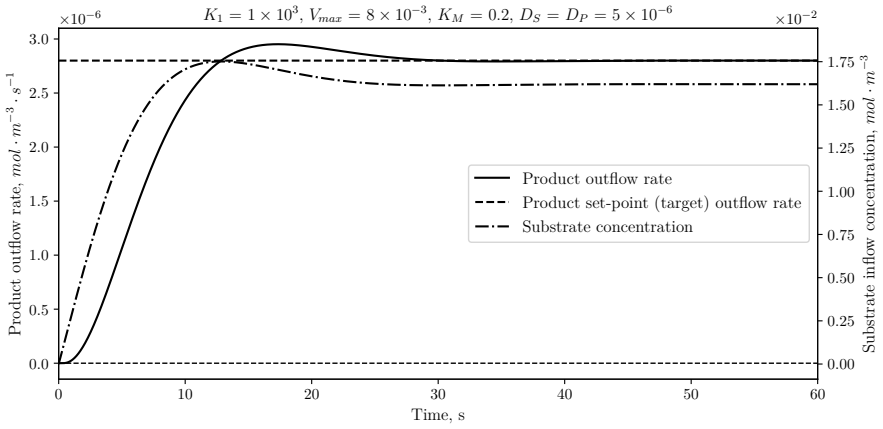

Figure 4.3: Control with adequate coefficients.

The second example here is the result displayed in the Fig. 4.4 which shows the influence of parameter K_c outside of the interval $(0, K_{c1})$ while all other parameters are the same as in the previous example (Fig 4.3). In this particular case, such selection of parameters yields unpredictable solutions as negative substrate concentrations in several points in time is observed. Another observable misbehavior are the periodic oscillations with an amplitude growth, thus the control target is not met. In this case, the control algorithm is not changed and should work as desired, but the chosen coefficient K_c gives this unpredictable result.

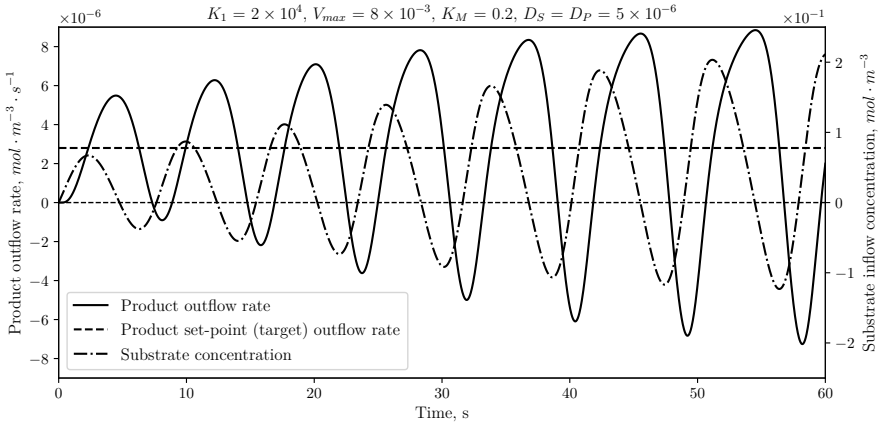

Figure 4.4: Control example with parameter K_c outside the interval $(0, K_{c1})$. Inflow substrate concentration is below zero at some point in time as well as the outflow rate.

Conclusions

The stability of the difference scheme for reaction-diffusion equation system has been analyzed. The essential feature of this problem is that a nonlocal boundary condition is formulated for a system of equations (for the first time, as far as the author is aware). The mathematical model is distinguished by the nonlocal boundary condition (4.10) which binds both derivatives w.r.t time $\partial S(d,t)/\partial t$ and space $\partial P/\partial x$.

An eigenvalue spectrum analysis for control and equation system parameters was carried out. The obtained results allow to choose the proper coefficients for the numerical algorithm with respect to difference scheme stability as well as the physical properties.

The computational results demonstrate the applicability of the integral control mechanism in bioreactor design. An integral control mechanism ("I" component from the PID controller) can be applied for a particular bioreactor design with monitoring.

The mathematical model could be applied for the treatment process modeling, where the patient needs to receive a strictly prescribed dose of the drug [41].

Conclusions

1. Proposed reaction–diffusion, convection–reaction–diffusion and convection–reaction mathematical models with nonlocal boundary and nonlocal conditions subject to PID control (or a subset of terms, PI, I) for bioreactor modeling have the potential to be applied in bioreactor modeling with a requirement for monitoring and control.

2. The reaction–diffusion mathematical model with a nonlocal boundary condition representing a PID controller has the potential to be applied in bioreactor modeling in drug delivery field.

3. The convection–reaction–diffusion system of PDEs with a control mechanism described using the nonlocal condition can be used for drug delivery mathematical modeling applied to the flow-through pressure controlled bioreactor.

4. The convection–reaction system of PDEs with a nonlocal condition for monitoring and control can be applied to the nitrate removal in a woodchip denitrification bioreactor with water flow rate monitoring.

5. A numerical algorithm was constructed and a computer program was developed. Sufficient conditions for numerical algorithm stability of difference scheme for the system of reaction–diffusion equations with the nonlocal boundary condition were obtained by using eigenvalue spectrum analysis for control and equation system parameters.

Bibliography

[1] V. Abet, F. Filace, J. Recio, J. Alvarez-Builla, and C. Burgos. Prodrug approach: An overview of recent cases. *European Journal of Medicinal Chemistry*, 127:810–827, 2017.

[2] K. Addy, A. J. Gold, L. E. Christianson, M. B. David, L. A. Schipper, and N. A. Ratigan. Denitrifying bioreactors for nitrate removal: A meta-analysis. *Journal of Environmental Quality*, 45(3):873–881, 2016.

[3] K. J. Aström and T. Hägglund. *PID Controllers: Theory, Design, and Tuning, Second Edition*. The Instrument, Systems, and Automation Society, Research Triangle Park, NC, 1995.

[4] K. J. Aström and T. Hägglund. *Advanced PID Control*, volume 461. ISA-The Instrumentation, Systems, and Automation Society Research Triangle Park, 2006.

[5] K. Atkinson. *An Introduction to Numerical Analysis*. Wiley, 1989. ISBN 9780471624899.

[6] R. Baronas, F. Ivanauskas, and J. Kulys. *Mathematical Modeling of Biosensors: An Introduction for Chemists and Mathematicians*, volume 9. Springer Science & Business Media, 2009.

[7] D. Blowes, W. Robertson, C. Ptacek, and C. Merkley. Removal of agricultural nitrate from tile-drainage effluent water using in-line bioreactors. *Journal of Contaminant Hydrology*, 15(3):207–221, 1994.

[8] R. Bürger, J. Careaga, S. Diehl, C. Mejías, I. Nopens, E. Torfs, and P. A. Vanrolleghem. Simulations of reactive settling of activated sludge with a reduced biokinetic model. *Computers & Chemical Engineering*, 92: 216–229, 2016.

[9] B. Cahlon, D. M. Kulkarni, and P. Shi. Stepwise stability for the heat equation with a nonlocal constraint. *SIAM Journal on Numerical Analysis*, 32(2):571–593, 1995.

[10] S. G. Cameron and L. A. Schipper. Nitrate removal and hydraulic performance of organic carbon for use in denitrification beds. *Ecological Engineering*, 36(11):1588–1595, 2010.

[11] J. Cannon. The solution of the heat equation subject to the specification of energy. *Quarterly of Applied Mathematics*, 21(2):155–160, 1963.

[12] J. Cannon and J. van der Hoek. Implicit finite difference scheme for the diffusion of mass in porous media. *Numerical Solution of Partial Differential Equations, North Holland*, pages 527–539, 1982.

[13] J. Cassidy, L. Frunzo, H. Lubberding, D. Villa-Gomez, G. Esposito, K. Keesman, and P. Lens. Role of microbial accumulation in biological sulphate reduction using lactate as electron donor in an inversed fluidized bed bioreactor: operation and dynamic mathematical modelling. *International Biodeterioration & Biodegradation*, 121:1–10, 2017.

[14] Y. Choi and K.-Y. Chan. A parabolic equation with nonlocal boundary conditions arising from electrochemistry. *Nonlinear Analysis: Theory, Methods & Applications*, 18(4):317–331, 1992.

[15] L. Christianson, A. Bhandari, and M. Helmers. Emerging technology: Denitrification bioreactors for nitrate reduction in agricultural waters. *Journal of Soil and Water Conservation*, 64(5):139A–141A, 2009.

[16] L. Christianson, A. Bhandari, and M. Helmers. Potential design methodology for agricultural drainage denitrification bioreactors. In *World Environmental and Water Resources Congress 2011: Bearing Knowledge for Sustainability*, pages 2740–2748, 2011.

[17] L. E. Christianson, A. Bhandari, and M. J. Helmers. Pilot-scale evaluation of denitrification drainage bioreactors: Reactor geometry and performance. *Journal of Environmental Engineering*, 137(4):213–220, 2011.

[18] L. E. Christianson, A. Bhandari, and M. J. Helmers. A practice-oriented review of woodchip bioreactors for subsurface agricultural drainage. *Applied Engineering in Agriculture*, 28(6):861–874, 2012.

[19] J. Chun, R. Cooke, J. Eheart, and J. Cho. Estimation of flow and transport parameters for woodchip-based bioreactors: II. field-scale bioreactor. *Biosystems Engineering*, 105(1):95–102, 2010.

[20] R. Čiegis, O. Suboč, and R. Čiegis. Numerical simulation of nonlocal delayed feedback controller for simple bioreactors. *Informatica*, 29(2): 233–249, 2018.

[21] R. Čiupaila, M. Sapagovas, and K. Pupalaigė. M-matrices and convergence of finite difference scheme for parabolic equation with integral boundary condition. *Mathematical Modelling and Analysis*, 25(2):167–183, 2020.

[22] L. Collatz. *Funktionalanalysis und Numerische Mathematik*. Berlin, 1964.

[23] R. Cooke, A. Doheny, and M. Hirschi. Bio-reactors for edge-of-field treatment of tile outflow. In *2001 ASAE Annual Meeting*. American Society

of Agricultural and Biological Engineers, 1998.

[24] W. Day. A decreasing property of solutions of parabolic equations with applications to thermoelasticity. *Quarterly of Applied Mathematics*, 40(4): 468–475, 1983.

[25] M. Dehghan. Efficient techniques for the second-order parabolic equation subject to nonlocal specifications. *Applied Numerical Mathematics*, 52(1): 39–62, 2005.

[26] G. Ekolin. Finite difference methods for a nonlocal boundary value problem for the heat equation. *BIT Numerical Mathematics*, 31(2):245–261, 1991.

[27] J. A. Eldridge, M. Milewski, A. L. Stinchcomb, and P. A. Crooks. Synthesis and in vitro stability of amino acid prodrugs of 6-β-naltrexol for microneedle-enhanced transdermal delivery. *Bioorganic & Medicinal Chemistry Letters*, 24(22):5212–5215, 2014.

[28] G. Ellis. *Control System Design Guide: Using Your Computer to Understand and Diagnose Feedback Controllers*. Butterworth-Heinemann, 2012.

[29] G. Fairweather and J. C. López-Marcos. Galerkin methods for a semilinear parabolic problem with nonlocal boundary conditions. *Advances in Computational Mathematics*, 6(1):243–262, 1996.

[30] G. W. Feyereisen, T. B. Moorman, L. E. Christianson, R. T. Venterea, J. A. Coulter, and U. W. Tschirner. Performance of agricultural residue media in laboratory denitrifying bioreactors at low temperatures. *Journal of Environmental Quality*, 45(3):779–787, 2016.

[31] C. M. Greenan, T. B. Moorman, T. B. Parkin, T. C. Kaspar, and D. B. Jaynes. Denitrification in wood chip bioreactors at different water flows. *Journal of Environmental Quality*, 38(4):1664–1671, 2009.

[32] A. Gulin. On the spectral stability in subspaces for difference schemes with nonlocal boundary conditions. *Differential Equations*, 49(7):815–823, 2013.

[33] A. Gulin, N. Ionkin, and V. Morozova. Study of the norm in stability problems for nonlocal difference schemes. *Differential Equations*, 42(7): 974–984, 2006.

[34] A. Gulin, V. Morozova, and N. Udovichenko. Stability of a nonlocal difference problem with a complex parameter. *Differential Equations*, 47 (8):1116, 2011.

[35] H. Gutfreund. *Kinetics for the Life Sciences: Receptors, Transmitters and*

Catalysts. Cambridge University Press, 1995.

[36] B. Hassanpour, S. Giri, W. T. Pluer, T. S. Steenhuis, and L. D. Geohring. Seasonal performance of denitrifying bioreactors in the northeastern united states: Field trials. *Journal of Environmental Management*, 202:242–253, 2017.

[37] N. L. Hoover, A. Bhandari, M. L. Soupir, and T. B. Moorman. Woodchip denitrification bioreactors: Impact of temperature and hydraulic retention time on nitrate removal. *Journal of Environmental Quality*, 45(3):803–812, 2016.

[38] N. Ionkin. Stability of a problem in heat transfert theory with nonclassical boundary condition. *Differential Equations*, 15(7):911–914, 1979.

[39] F. Ivanauskas, T. Meškauskas, and M. Sapagovas. Stability of difference schemes for two-dimensional parabolic equations with non-local boundary conditions. *Applied Mathematics and Computation*, 215(7):2716–2732, 2009.

[40] F. Ivanauskas, Y. Novitski, and M. Sapagovas. On the stability of an explicit difference scheme for hyperbolic equations with nonlocal boundary conditions. *Differential Equations*, 49(7):849–856, 2013.

[41] F. Ivanauskas, V. Laurinavičius, M. Sapagovas, and A. Nečiporenko. Reaction–diffusion equation with nonlocal boundary condition subject to pid-controlled bioreactor. *Nonlinear Analysis: Modelling and Control*, 22 (2):261–272, 2017.

[42] F. Ivanauskas, V. Laurinavičius, M. Sapagovas, and A. Nečiporenko. Reaction–diffusion equation with nonlocal boundary condition subject to PID-controlled bioreactor. *Nonlinear Analysis: Modelling and Control*, 22 (2):261–272, 2017. doi: 10.15388/NA.2017.2.9.

[43] J. Jachimaviciene, M. Sapagovas, A. Štikonas, and O. Štikoniene. On the stability of explicit finite difference schemes for a pseudoparabolic equation with nonlocal conditions. *Nonlinear Analysis: Modelling and Control*, 19 (2):225–240, 2014.

[44] G. Kalna and S. McKee. The thermostat problem with a nonlocal nonlinear boundary condition. *IMA Journal of Applied Mathematics*, 69(5):437–462, 2004.

[45] L. Kamynin. A boundary value problem in the theory of heat conduction with a nonclassical boundary condition. *USSR Computational Mathematics and Mathematical Physics*, 4(6):33 – 59, 1964. ISSN 0041-5553.

[46] V. Kamynin. On the inverse problem of determining the right-hand side

of a parabolic equation under an integral overdetermination condition. *Mathematical Notes*, 77(3-4):482–493, 2005.

[47] O. Khan, C. M. R. Madhuranthakam, P. Douglas, H. Lau, J. Sun, and P. Farrell. Optimized PID controller for an industrial biological fermentation process. *Journal of Process Control*, 71:75–89, 2018. ISSN 0959-1524.

[48] M. King et al. *Process Control: A Practical Approach*. Wiley Online Library, 2011.

[49] M. J. Kochenderfer and T. A. Wheeler. *Algorithms for Optimization*. MIT Press, 2019.

[50] J. Kulys. Biosensor response at mixed enzyme kinetics and external diffusion limitation in case of substrate inhibition. *Nonlinear Analysis: Modelling and Control*, 11(4):385–392, 2006.

[51] J. Kulys and R. Baronas. Modelling of amperometric biosensors in the case of substrate inhibition. *Sensors*, 6(11):1513–1522, 2006.

[52] S. V. Kumar, D. Saravanan, B. Kumar, and A. Jayakumar. An update on prodrugs from natural products. *Asian Pacific Journal of Tropical Medicine*, 7:S54–S59, 2014.

[53] V. Laurinavicius, J. Razumiene, A. Ramanavicius, and A. D. Ryabov. Wiring of PQQ–dehydrogenases. *Biosensors and Bioelectronics*, 20(6): 1217 – 1222, 2004. ISSN 0956-5663. Special Issue on Synthetic Receptors.

[54] V. Laurinavičius, F. Ivanauskas, and A. Nečiporenko. Drug delivery mathematical modeling for pressure controlled bioreactor. *Journal of Mathematical Chemistry*, 57(8):1973–1982, 2019.

[55] K. Lee, Y. Choi, B. S. Lee, and K. Nam. Differential mode of denitrification by pseudomonas sp. KY1 using molasses as a carbon source. *KSCE Journal of Civil Engineering*, 21(6):2097–2105, 2017.

[56] H. Lei, I. Nahum-Shani, K. Lynch, D. Oslin, and S. Murphy. A "smart" design for building individualized treatment sequences. *Annual Review of Clinical Psychology*, 8(1):21–48, 2012.

[57] T. Leonavičienė, A. Bugajev, G. Jankevičiūtė, and R. Čiegis. On stability analysis of finite difference schemes for generalized kuramoto-tsuzuki equation with nonlocal boundary conditions. *Mathematical Modelling and Analysis*, 21(5):630–643, 2016.

[58] C. Lepine, L. Christianson, K. Sharrer, and S. Summerfelt. Optimizing hydraulic retention times in denitrifying woodchip bioreactors treating recirculating aquaculture system wastewater. *Journal of Environmental Quality*, 45(3):813–821, 2016.

[59] S. B. Leschine. Cellulose degradation in anaerobic environments. *Annual Review of Microbiology*, 49(1):399–426, 1995.

[60] Y. Lin. Analytical and numerical solutions for a class of nonlocal nonlinear parabolic differential equations. *SIAM Journal on Mathematical Analysis*, 25(6):1577–1594, 1994.

[61] T. Liu, X. Yuan, T. Jia, C. Liu, Z. Ni, Z. Qin, and Y. Yuan. Polymeric prodrug of bufalin for increasing solubility and stability: Synthesis and anticancer study in vitro and in vivo. *International Journal of Pharmaceutics*, 506(1):382–393, 2016.

[62] J. Martín-Vaquero and J. Vigo-Aguiar. On the numerical solution of the heat conduction equations subject to nonlocal conditions. *Applied Numerical Mathematics*, 59(10):2507–2514, 2009.

[63] J. Martín-Vaquero, A. Queiruga-Dios, and A. H. Encinas. Numerical algorithms for diffusion–reaction problems with non-classical conditions. *Applied Mathematics and Computation*, 218(9):5487–5495, 2012.

[64] T. Murakami. A minireview: Usefulness of transporter-targeted prodrugs in enhancing membrane permeability. *Journal of Pharmaceutical Sciences*, 105(9):2515–2526, 2016.

[65] A. M. Nakhushev. Equations of mathematical biology (in Russian). *Vysshaya Shkola, Moscow*, 1:995, 1995.

[66] D. D. N'Da. Prodrug strategies for enhancing the percutaneous absorption of drugs. *Molecules*, 19(12):20780–20807, 2014.

[67] C. Pao. Numerical solutions of reaction–diffusion equations with nonlocal boundary conditions. *Journal of Computational and Applied Mathematics*, 136(1-2):227–243, 2001.

[68] R. S. Parker and F. J. Doyle. Control-relevant modeling in drug delivery. *Advanced Drug Delivery Reviews*, 48(2):211–228, 2001.

[69] S. Peciulyte, O. Štikoniene, and A. Štikonas. Investigation of negative critical points of the characteristic function for problems with nonlocal boundary conditions. *Nonlinear Analysis: Modelling and Control*, 13(4): 467–490, 2008.

[70] N. A. Peppas and B. Narasimhan. Mathematical models in drug delivery: How modeling has shaped the way we design new drug delivery systems. *Journal of Controlled Release*, 190:75 – 81, 2014. ISSN 0168-3659. doi: 10.1016/j.jconrel.2014.06.041. 30th Anniversary Special Issue.

[71] M. Picone. Su un problema al contorno nelle equazioni differenziali lineari ordinarie del secondo ordine. *Annali della Scuola Normale Superiore di*

Pisa-Classe di Scienze, 10:1–95, 1908.

[72] A. Povilaitis and J. Matikienė. Nitrate removal from tile drainage water: The performance of denitrifying woodchip bioreactors amended with activated carbon and flaxseed cake. *Agricultural Water Management*, 229: 105937, 2020. ISSN 0378-3774.

[73] A. Povilaitis, A. Rudzianskaite, S. Miseviciene, V. Gasiunas, O. Miseckaite, and I. Živatkauskiene. Efficiency of drainage practices for improving water quality in Lithuania. *Transactions of the ASABE*, 61(1):179–196, 2018.

[74] J. Rautio, H. Kumpulainen, T. Heimbach, R. Oliyai, D. Oh, T. Järvinen, and J. Savolainen. Prodrugs: design and clinical applications. *Nature Reviews Drug Discovery*, 7(3):255–270, 2008.

[75] A. Samarskii and A. Gulin. *Numerical Methods (in Russian)*. Nauka, Moscow, 1989.

[76] A. A. Samarskii. *The Theory of Difference Schemes*, volume 240. Marcel Dekker New York, 2001.

[77] M. Sapagovas. On the stability of a finite-difference scheme for nonlocal parabolic boundary-value problems. *Lithuanian Mathematical Journal*, 48 (3):339–356, 2008.

[78] M. Sapagovas, T. Meškauskas, and F. Ivanauskas. Numerical spectral analysis of a difference operator with non-local boundary conditions. *Applied Mathematics and Computation*, 218(14):7515–7527, 2012.

[79] M. Sapagovas, R. Čiupaila, Ž. Jokšienė, and T. Meškauskas. Computational experiment for stability analysis of difference schemes with nonlocal conditions. *Informatica*, 24(2):275–290, 2013.

[80] M. Sapagovas, T. Meškauskas, and F. Ivanauskas. Influence of complex coefficients on the stability of difference scheme for parabolic equations with non-local conditions. *Applied Mathematics and Computation*, 332: 228–240, 2018.

[81] M. Sapagovas, R. Čiupaila, K. Jakubėlienė, and S. Rutkauskas. A new eigenvalue problem for the difference operator with nonlocal conditions. *Nonlinear Analysis: Modelling and Control*, 24(3):462–484, Apr. 2019.

[82] L. A. Schipper, W. D. Robertson, A. J. Gold, D. B. Jaynes, and S. C. Cameron. Denitrifying bioreactors—an approach for reducing nitrate loads to receiving waters. *Ecological Engineering*, 36(11):1532–1543, 2010.

[83] K. Schügerl. *Bioreaction Engineering: Reactions Involving Microorganisms and Cells*. Wiley New York, 1987.

[84] J. Siepmann and N. Peppas. Mathematical modeling of controlled drug delivery. *Advanced Drug Delivery Reviews*, 48(2-3):137–300, 2001. ISSN 0169-409X. doi: 10.1016/S0169-409X(01)00111-9.

[85] A. Štikonas. A survey on stationary problems, Green's functions and spectrum of Sturm–Liouville problem with nonlocal boundary conditions. *Nonlinear Analysis: Modelling and Control*, 19(3):301–334, 2014.

[86] J. Tamarkin. On some general problems of the theory of ordinary linear differential operators and the expansion of arbitrary functions into series, 1917 (in Russian).

[87] I. Tinoco, K. Sauer, J. C. Wang, J. D. Puglisi, G. Harbison, and D. Rovnyak. *Physical Chemistry: Principles and Applications in Biological Sciences*, volume 545. Prentice Hall New Jersey, 1995.

[88] A. Turner, I. Karube, and G. S. Wilson. *Biosensors: Fundamentals and Applications*. Oxford University Press, 1987.

[89] P. Van Driel, W. Robertson, and L. Merkley. Denitrification of agricultural drainage using wood-based reactors. *Transactions of the ASABE*, 49(2): 565–573, 2006.

[90] S. Verma, R. Bhattarai, R. Cooke, J. A. Chun, and G. E. Goodwin. Evaluation of conservation drainage systems in illinois–bioreactors. In *2010 Pittsburgh, Pennsylvania, June 20-June 23, 2010*. American Society of Agricultural and Biological Engineers, 2010.

[91] W. Wang, M. Yamamoto, and B. Han. Two-dimensional parabolic inverse source problem with final overdetermination in reproducing kernel space. *Chinese Annals of Mathematics, Series B*, 35(3):469–482, 2014.

[92] W. Whyburn. Differential equations with general boundary conditions. *Bulletin of the American Mathematical Society*, 48(10):692–704, 1942.

[93] Y.-h. Yang, H. Aloysius, D. Inoyama, Y. Chen, and L.-q. Hu. Enzyme-mediated hydrolytic activation of prodrugs. *Acta Pharmaceutica Sinica B*, 1(3):143–159, 2011.

Publications by the Author

Articles in journals indexed in the Claritive Analytics Web of Science:

[A1] F. Ivanauskas, V. Laurinavičius, M. Sapagovas, and **A. Nečiporenko**. Reaction–diffusion equation with nonlocal boundary condition subject to PID-controlled bioreactor. *Nonlinear Analysis: Modelling and Control*, 22(2):261-272, 2017, Vilnius University.

[A2] V. Laurinavičius, F. Ivanauskas and **A. Nečiporenko**. Drug delivery mathematical modeling for pressure controlled bioreactor. *Journal of Mathematical Chemistry*, 57(8):1973-1982, 2019, Springer.

Articles in International conference proceedings

[A3] **A. Nečiporenko**, F. Ivanauskas, V. Laurinavičius, M. Sapagovas. PID-controlled flow-through bioreactor *30th Nordic Seminar on Computational Mechanics*, Technical University of Denmark, Lyngby, Denmark. 2017, p. 133-136

[A4] **A. Nečiporenko**, F. Ivanauskas, V. Laurinavičius, M. Sapagovas. PID-controlled drug delivery system subject to flow-through bioreactor *3rd NESUS Winter School and PhD Symposium 2018*, Ruđer Bošković Institute, Zagreb, Croatia. 2018, vol. 1, no. 1, p. 13.

Anatolij Nečiporenko

MATHEMATICAL MODELING OF BIOREACTOR CONTROL

Doctoral Dissertation
Natural Sciences
Informatics N 009
Editor: Daiva Klipšaitė

Vilnius University Press
9 Saulėtekio Ave., Building III, LT-10222 Vilnius
Email: info@leidykla.vu.lt, www.leidykla.vu.lt
Print run copies 20